Clim. Past Discuss., 7, 3239–3286, 2011
www.clim-past-discuss.net/7/3239/2011/
doi:10.5194/cpd-7-3239-2011

Climate of the Past Discussions

Persistent influence of ice sheet melting on high northern latitude climate during the early Last Interglacial

A. Govin[1,*], **P. Braconnot**[1], **E. Capron**[1,**], **E. Cortijo**[1], **J.-C. Duplessy**[1], **E. Jansen**[2], **L. Labeyrie**[1], **A. Landais**[1], **O. Marti**[1], **E. Michel**[1], **E. Mosquet**[1], **B. Risebrobakken**[2], **D. Swingedouw**[1], and **C. Waelbroeck**[1]

[1]LSCE/IPSL Laboratoire des Sciences du Climat et de l'Environnement, UMR8212, CEA-CNRS-UVSQ, Gif sur Yvette, France
[2]Bjerknes Centre for Climate Research, University of Bergen, Bergen, Norway
[*]now at: MARUM/Center for Marine Environmental Sciences, University of Bremen, Leobener Strasse, Bremen, Germany
[**]now at: British Antarctic Survey, High Cross, Madingley Road, Cambridge, CB3 0ET, UK

Received: 3 October 2011 – Accepted: 5 October 2011 – Published: 11 October 2011

Correspondence to: A. Govin (aline.govin@uni-bremen.de)

Published by Copernicus Publications on behalf of the European Geosciences Union.

Abstract

Although the Last Interglacial (LIG) is often considered as a possible analogue for future climate in high latitudes, its precise climate evolution and associated causes remain uncertain. Here we compile high-resolution marine sediment records from the North Atlantic, Labrador Sea, Norwegian Sea and the Southern Ocean. We document a delay in the establishment of peak interglacial conditions in the North Atlantic, Labrador and Norwegian Seas as compared to the Southern Ocean. In particular, we observe a persistent iceberg melting at high northern latitudes at the beginning of the LIG. It suggests that the input of meltwater has maintained (1) colder and fresher surface-water conditions in the North Atlantic, Labrador and Norwegian Seas and (2) weaker ventilation of North Atlantic deep waters during the early LIG (129–125.5 ka) compared to the late LIG. Results from an ocean-atmosphere coupled model with insolation as a sole forcing for three key periods of the LIG show that insolation variations alone lead to warmer North Atlantic surface waters and stronger Atlantic overturning during the early LIG (126 ka) than the late LIG (122 ka). Hence insolation variations alone do not explain the delay in peak interglacial conditions observed at high northern latitudes. When freshwater input is interactively computed at 126 ka in response to the high boreal summer insolation, the model simulates colder, fresher North Atlantic surface waters and weaker Atlantic overturning during the early LIG (126 ka) compared to the late LIG (122 ka). This result indicates that both insolation variations and ice sheet melting have to be considered to reproduce the LIG climate evolution and supports our hypothesis that optimal thermal and deep ocean circulation conditions at high northern latitudes develop during the late LIG only, when the freshwater supply has already ceased.

1 Introduction

The Last Interglacial (LIG) period (129–118 ka, 1 ka = 1000 years) is also termed Marine Isotope Stage 5.5 (MIS 5.5) in marine sediment cores or Eemian in European continental records (e.g. Kukla et al., 1997, 2002). This period is characterized by a high-latitude climate warmer by several degrees than today (North Greenland Ice Core Project members, 2004; Cape Last Interglacial Project members, 2006; EPICA Community members, 2006; Clark and Huybers, 2009). Sea level was at least 6 m above the present level (Kopp et al., 2009) due to smaller glacier ice volume (e.g. Koerner, 1989; Otto-Bliesner et al., 2006) in response to the high boreal summer insolation (e.g. Berger and Loutre, 1991). Given its high insolation forcing, the LIG is generally regarded as a potential analogue for future climate evolution (e.g. Kukla et al., 2002; Jansen et al., 2007).

Characterized by extreme seasonal variations in temperature-sensitive processes (e.g. sea ice extent) and large-scale feedbacks mechanisms, polar regions are particularly sensitive to variations in climate forcing and are expected to experience large environmental changes in the near future (Meehl et al., 2007). The sequence of variations in the surface and deep oceans is well documented at high northern and southern latitudes during the last deglaciation (Termination I, see Denton et al., 2010 for a review). Most marine records from the North Atlantic and the Nordic Seas indicate an early to mid-Holocene (~10–8 ka) oceanic thermal optimum (e.g. Birks and Koç, 2002; Calvo et al., 2002; Hald et al., 2007; Bauch and Erlenkeuser, 2008; Andersson et al., 2010; Risebrobakken et al., 2011), in agreement with maximum boreal summer insolation values recorded at 11 ka (e.g. Berger and Loutre, 1991). Similarly, high southern latitudes exhibit high temperatures as early as 11.7 ka in the Southern Ocean (e.g. Calvo et al., 2007; Skinner et al., 2010) and over Antarctica (e.g. EPICA Community members, 2006; Stenni et al., 2011). In contrast, sea level rose of ca 60 m during the early Holocene until 7 ka when the Holocene sea level highstand was reached (e.g. Smith et al., 2011 for a review).

CPD
7, 3239–3286, 2011

The deglacial history of the penultimate deglaciation (Termination II) is less documented. For example, discrepancies exist between marine records on the existence of a northern temperature reversal during Termination II (Sarnthein and Tiedemann, 1990; Adkins et al., 1997; Chapman and Shackleton, 1998; Oppo et al., 2001; Kelly et al., 2006; Desprat et al., 2007; Weldeab et al., 2007). The establishment of the peak interglacial warmth at high northern latitudes during the LIG also remains controversial. Some studies showed evidence for an early LIG development of peak interglacial conditions in the Norwegian Sea and a later climatic optimum at mid latitudes in the North Atlantic (Cortijo et al., 1994, 1999). In contrast, other studies highlighted an early warming phase in the North Atlantic during the LIG (Rasmussen et al., 2003b; Bauch and Kandiano, 2007) and a late warming phase in the Norwegian Sea (Fronval and Jansen, 1997; Fronval et al., 1998; Rasmussen et al., 2003b). Part of these discrepancies arise from the difficulty of (1) collecting marine sediment cores from the Nordic Seas with high sedimentation rates during the LIG, and (2) defining reliable stratigraphical time frames between the North Atlantic and the Nordic Seas during the LIG (e.g. Fronval and Jansen, 1997; Cortijo et al., 1999; Rasmussen et al., 2003b; Risebrobakken et al., 2005, 2006; Bauch and Erlenkeuser, 2008).

Recent high-resolution Norwegian Sea records suggest that the LIG thermal optimum in the Norwegian Sea occurred relatively late after the penultimate deglaciation (Bauch and Erlenkeuser, 2008; Bauch et al., 2011; Van Nieuwenhove et al., 2011), at a time when the boreal summer insolation was already significantly reduced (e.g. Berger and Loutre, 1991). They also show that the LIG peak warmth in the Norwegian Sea never reached the high warmth level of the early Holocene (Bauch and Erlenkeuser, 2008; Bauch et al., 2011), although the boreal summer insolation at the beginning of the LIG was higher by $20\,\mathrm{W\,m^{-2}}$ than during the early Holocene. These results indicate that the temperature evolution in the Nordic Seas was not only a direct response to insolation variations during the LIG, in opposition to the early Holocene (Bauch et al., 2011).

CPD
7, 3239–3286, 2011

The Late Saalian glacial period preceding the LIG was a prolonged cold period in Europe characterized by a large Eurasian ice sheet that extended from the Norwegian shelf to the Barents-Kara Sea further south than any subsequent glacial episode (e.g. Svendsen et al., 2004). The Eurasian Saalian ice sheet retreated relatively quickly during Termination II. For example, grounded ice remained only on northern Scandinavia, the present Kara Sea and Arctic islands at ca. 134 ka (Lambeck et al., 2006). High boreal summer insolation explains the rapidity of northern ice sheet retreat during the penultimate deglaciation (Ruddiman et al., 1980). This fast ice sheet melting, which induced high meltwater discharge (Carlson, 2008) and reduced Atlantic Meridional Overturning Circulation (AMOC) throughout the deglaciation (Oppo et al., 1997), also likely explains the absence of a Younger Dryas-like event during Termination II (Ruddiman et al., 1980; Carlson, 2008). Uncertainties however remain on the timing of the LIG sea level highstand ranging from around 129 ka to around 124 ka (Cutler et al., 2003; Siddall et al., 2003; Thompson and Goldstein, 2006; Rohling et al., 2008; Waelbroeck et al., 2008; Blanchon et al., 2009). Hence continued melting from the Eurasian Saalian ice sheet at the beginning of the LIG may have contributed to the delay in peak interglacial warmth recently documented in the Norwegian Sea (Bauch et al., 2011; Van Nieuwenhove et al., 2011).

The objectives of this study are twofold. First we investigate the geographical polar extension of the late thermal optimum recorded in Norwegian Sea surface waters during the LIG and its potential counterpart in deep waters. For that purpose, we compiled five high-resolution marine sediment records from the North Atlantic, Labrador Sea and Norwegian Sea that we compare with a sediment record from the Southern Ocean, taken as a reference for high southern latitude climate. We define a consistent time frame between the Norwegian Sea, Labrador Sea, the North Atlantic and Southern Ocean during the LIG and compare the timing of establishment of high-latitude peak interglacial conditions recorded by surface and deep waters. Second, we use a coupled ocean-atmosphere General Circulation Model to investigate the plausible causes (insolation changes versus meltwater input) responsible for the late oceanic climate optimum observed at high northern latitudes during the LIG. We discuss the results of the model simulations performed for three key periods of the LIG and the limits of the model-data intercomparison.

2 Material and methods

2.1 Marine sediment cores and analyses

We selected six marine sediment cores with a relatively high sedimentation rate (ranging from ~5 to 17 cm ka^{-1}) during the LIG (see Table 1 for the name and references of the cores). We chose three cores in the North Atlantic located at increasing water-depths from 2000 m to 4000 m (Table 1). The core locations presently lie in North Atlantic Deep Waters (NADW). We completed this dataset with two sediment cores collected from basins of modern deep-water formation: one in the Norwegian Sea and one in the Labrador Sea (Table 1). Finally, we chose one sediment core from the Indian sector of the Southern Ocean as a reference for the LIG climate evolution in southern subpolar regions (Table 1). Complementary proxies (foraminiferal stable isotope analyses, Sea Surface Temperature and Ice-Rafted Detritus reconstructions) are available in these cores during our period of interest (132–115 ka).

All discussed cores present high-resolution oxygen and carbon isotopic (δ^{18}O and δ^{13}C) records obtained on both planktic and benthic foraminifera. Foraminiferal δ^{18}O and δ^{13}C analyses are expressed in ‰ versus Vienna PDB, defined with respect to NBS 19 calcite standard (δ^{18}O = −2.20 ‰ and δ^{13}C = + 1,95 ‰). We present the benthic δ^{18}O data on the *Uvigerina* scale and show δ^{13}C data measured on the epibenthic *Cibicides* genus only. We increased the resolution of the benthic foraminiferal isotopic record from the Southern Ocean core reported by Govin et al. (2009) and generated a benthic record with a resolution better than 0.5 ka over the entire period 130–115 ka.

Reconstructions of summer Sea Surface Temperatures (SST) are exclusively based on faunal assemblages of foraminifera in the North Atlantic and Southern Ocean cores for higher consistency. We increased the resolution of SST data from the Southern Ocean core to an averaged resolution of 0.4 ka during the LIG, following the methodology described in Govin et al. (2009). In the Norwegian and Labrador Sea cores, SST estimates are originally based on the percentage of the polar foraminifera species *Neogloboquadrina pachyderma* sinistral. To generate consistent SST records at high northern latitudes, we converted the percentages of *N. pachyderma* sinistral of the Labrador and Norwegian Sea cores into summer SST and calculated the linear relationship linking summer SST and the percentage of *N. pachyderma* sinistral at high northern latitudes in the 6 to 12 °C range (Fig. 1). Ice Rafted Detritus (IRD) data are expressed as the number of lithic grains per gram of dry sediment. IRD > 150 µm were counted in the North Atlantic cores, whereas IRD > 500 µm were counted in the Norwegian Sea core.

Finally, we reconstructed seawater δ^{18}O ($\delta^{18}O_{sw}$) variations in the North Atlantic cores CH69-K09 and ODP 980. We calculated $\delta^{18}O_{sw}$ values as the residual (Shackleton, 1974; Duplessy et al., 1991) between the planktic δ^{18}O records (from *Globigerina bulloides* and *N. pachyderma* sinistral in core CH69-K09; from *N. pachyderma* dextral in core ODP 980) and SST records. For both cores, $\delta^{18}O_{sw}$ data are presented relatively to the averaged Late Holocene $\delta^{18}O_{sw}$ value that we calculated for the last 3.5 ka (0.73 ‰ SMOW in core CH69-K09 and 0.38 ‰ SMOW in core ODP 980). Given the uncertainties on the timing of the LIG sea level highstand and the relatively small amplitude of sea level variations (<10 m) during the LIG (e.g. Waelbroeck et al., 2002; Thompson and Goldstein, 2006; Rohling et al., 2008; Blanchon et al., 2009), we do not correct here the $\delta^{18}O_{sw}$ values for ice volume variations.

CPD
7, 3239–3286, 2011

2.2 Model simulations

To gain insight on the climate forcing and processes responsible for the late LIG oceanic optimum observed at high northern latitudes, we use model simulations performed with the coupled ocean-atmosphere General Circulation Model (GCM) IPSL-CM4 (Marti et al., 2010). We consider the model outputs of a series of simulations performed for three time slices of the LIG (see Table 2 for a summary). Model simulations were forced with insolation values from Berger (1978) and the modern ice sheet configuration (Braconnot et al., 2008). The Greenland ice sheet (GIS) is hence the only northern ice sheet represented in the model.

We investigate the LIG response of high northern latitude climate to two different types of perturbation: (1) response to insolation variations only and (2) additional impact of a northern meltwater input. First, to study the effect of insolation variations on high northern latitude climate during the LIG, we use the results of simulations performed for three key periods of the LIG characterized by distinct insolation values (Braconnot et al., 2008): maximum in boreal summer insolation in the early LIG at 126 ka (250 year-long simulation), intermediate insolation values in the mid LIG at 122 ka (800 year-long simulation), and minimum in boreal summer insolation at 115 ka (700 year-long simulation) (Table 2).

Second, to investigate the influence of a northern meltwater input on high-latitude climate during the early LIG, we consider two simulations at 126 ka. In addition to the 126 ka simulation described above, which integrates the direct climatic response to insolation forcing at 126 ka (Braconnot et al., 2008), we add, in a second simulation called "126 ka meltwater" (Table 2), the response of ice caps (here the melting of Greenland) by using the simple parameterization developed for future climate (Swingedouw et al., 2007a, 2009). The novelty here, when compared to classical freshwater experiments, is that (1) the influence of the specific 126 ka insolation values on the LIG climate is taken into account, and (2) the meltwater flux is interactive with climate (Swingedouw et al., 2007a, 2009). In response to the high boreal summer insolation

CPD
7, 3239–3286, 2011

at 126 ka, about 0.17 Sv freshwater flux is redistributed in the North Atlantic north of 40°N. Because this number is high as compared to other estimates (Otto-Bliesner et al., 2006), the "126 ka meltwater" simulation represents the highest effect that a meltwater pulse could have on high northern latitude climate during the early LIG and does not pretend to represent the real climate at 126 ka (see Sect. 4.3.2).

3 Marine records: evolution of the LIG climate

3.1 Establishment of the interhemispheric time frame

The definition of reliable chronologies is critical to compare the LIG climate evolution indicated by records from different water depths and oceanic basins. Direct correlation of the plateau of benthic δ^{18}O minimum values (hereafter called benthic O-plateau) is commonly applied during the LIG (e.g. Cortijo et al., 1999). Benthic δ^{18}O data however do not only reflect global ice volume variations because they are also affected by deep-water temperature changes (e.g. Skinner and Shackleton, 2005), the presence of ^{18}O-depleted deep waters in the Nordic Seas (e.g. Dokken and Jansen, 1999; Risebrobakken et al., 2006; Bauch and Erlenkeuser, 2008), that may reach the deep North Atlantic (Labeyrie et al., 2005; Waelbroeck et al., 2006, 2011), and/or the injection of ^{18}O-depleted meltwater (Ganopolski and Roche, 2009). We prefer to develop here a common time frame between sediment cores from the Labrador and Norwegian Seas, the North Atlantic and Southern Ocean during the LIG that is independent from benthic isotope stratigraphy (e.g. Skinner et al., 2010; Waelbroeck et al., 2011). We transfer the marine sediment records on one single time scale, and use the most recent (EDC3) chronology available for the Antarctic EPICA Dome C (EDC) and Dronning Maud Land (EDML) ice cores during the LIG (Loulergue et al., 2007; Parrenin et al., 2007; Ruth et al., 2007). This chronology has been extended to the Greenland ice core at North-GRIP (North Greenland Ice Core Project members, 2004) during the LIG, using global atmospheric markers (Capron et al., 2010).

3.1.1 Age models of the Southern Ocean and North Atlantic cores

To transfer the Southern Ocean and North Atlantic records on this timescale, we assume that surface-water temperature changes in the subantarctic zone of the Southern Ocean (respectively in the North Atlantic) occurred simultaneously with air temperature variations over inland Antarctica (respectively Greenland). This has in particular been observed during the last glacial period and Termination I (e.g. Bond et al., 1993; Calvo et al., 2007).

Southern Ocean core

We tied the SST record from core MD02-2488 to the deuterium record from the EDC ice core (Jouzel et al., 2007). Because the SST resolution of the Southern Ocean core has been increased since the publication by Govin et al. (2009), we adjusted the original age model by up to 2 ka during the LIG period. Figure 2 presents the new age model. The tie-points defined and associated age uncertainties are given in Table 3. Tie-points are defined as follows. We synchronized the first increase in SST and deuterium recorded in the marine and ice cores at the beginning of Termination II (Fig. 2). The accelerated temperature increases observed between small "temperature plateaux" in EDC deuterium record during Termination II are tied to similar events recorded in core MD02-2488 (Fig. 2). We synchronized the SST and deuterium maxima from the marine and ice cores at the beginning of the LIG, and the beginning of the SST and deuterium decrease from both cores at the end of the LIG (Fig. 2). Finally, the age model during the last glacial inception relies on three tie-points: at midpoint, by the temperature minimum preceding the warm phase of Dansgaard-Oeschger (D/O) event 25, and by the temperature minimum defined between the warm phases of D/O 25 and 24 (Fig. 2).

North Atlantic cores

We synchronized the SST proxy records from the North Atlantic cores ODP 980, MD95-2042 and CH69-K09 to the ice $\delta^{18}O$ record from NGRIP Greenland ice core during the last glacial inception (Fig. 3). Note that the planktic *Globigerina bulloides* $\delta^{18}O$ record is a good proxy of SST in core MD95-2042 (Shackleton et al., 2000). The Greenland ice core however does not cover the early LIG (North Greenland Ice Core Project members, 2004). We assume that, like Termination I (Severinghaus et al., 1998), the abrupt warming of the air above Greenland during Termination II is synchronous with the global abrupt increase in methane recorded in the Antarctic ice core (Loulergue et al., 2008). We hence tied the North Atlantic SST proxy records to EDC methane record during Termination II (Fig. 3). We defined the tie-points as follows (Table 3). At the beginning of the LIG, the final SST increase recorded in the marine cores is synchronized to the abrupt methane increase recorded in the Antarctic ice core (Fig. 3). At the end of the LIG, the first pronounced North Atlantic cooling (related to the cold event 26, Oppo et al., 2006) is tied to the corresponding enhanced cooling recorded in the Greenland ice core (Fig. 3). We finally synchronized surface-water and air temperature changes at the beginning or the end of D/O 25 during the last glacial inception (Fig. 3). Altogether the three North Atlantic cores present, within age uncertainties (Table 3), consistent benthic $\delta^{18}O$ variations during the period 135–110 ka (see Fig. 6).

The maximum age uncertainty between the Southern Ocean and North Atlantic cores is estimated to be ±2.6 ka (1 σ) over the period 130–115 ka (see Table 3 for details). Within this time frame, the benthic O-plateau, which marks interglacial periods in marine sediment cores (Shackleton, 1969), starts at around 129.7 ka (±0.6 ka) in the North Atlantic, i.e. 3.3 ± 2.6 ka earlier than in the Southern Ocean (Figs. 5a and 6a). This offset is consistent with time-lags observed within the deep ocean during deglaciations (Bard et al., 1991; Skinner and Shackleton, 2005; Ganopolski and Roche, 2009).

CPD
7, 3239–3286, 2011

3.1.2 Age models of the Labrador Sea and Norwegian Sea cores

Defining reliable chronologies to sediment cores from the Labrador and Norwegian Seas is complicated by two facts. (1) SST variations below 6 °C are not recorded by changes in the percentage of *N. pachyderma* sinistral (Fig. 1), which dominates foraminifera faunal assemblages during cold periods. The timing and amplitude of the temperature increase during Termination II are hence not well defined in the Labrador and Norwegian Seas. (2) Planktic and benthic δ^{18}O records are strongly affected by ^{18}O-depleted waters during Termination II (e.g. Risebrobakken et al., 2006; Bauch and Erlenkeuser, 2008). The beginning of the LIG benthic O-plateau is thus not clearly defined in the Labrador and Norwegian Seas.

Labrador Sea core

To define the age model of core EW9302-JPC2 (Fig. 4, left panel) at the beginning of the LIG, we assume that the beginning of the surface-water warming in the Labrador Sea occurred simultaneously with the abrupt increase in methane recorded in the Antarctic ice core (Fig. 4a–b, Table 3). The upper limit of the diatom layer (grey-shaded area in Fig. 4) hence marks the onset of the LIG at ∼128.8 ka, similarly to the beginning of the Holocene (Rasmussen et al., 2003a). In addition, the deglacial melting signal indicated by low benthic δ^{18}O values during Termination II (Rasmussen et al., 2003a) ends, within age uncertainties, at the beginning of the North Atlantic benthic O-plateau (Fig. 4). At the end of the LIG, we tied the midpoint of the cooling transition (indicated by increasing percentages of *N. pachyderma* sinistral) to the enhanced cooling recorded in NGRIP δ^{18}O record (Fig. 4a–b). Consistent benthic δ^{18}O variations in the Labrador Sea and North Atlantic after ∼120 ka supports this approach (Fig. 4c). The maximum age uncertainty on records from the Labrador Sea is estimated to be ±2.3 ka (1 σ) over the period 130–115 ka (Table 3).

CPD
7, 3239–3286, 2011

Norwegian Sea core

Similarly to the Labrador Sea, we synchronized at the beginning of the LIG the beginning of the surface-water warming in the Norwegian Sea core MD95-2010 (Fig. 4, right panel) with the abrupt increase in methane recorded in the Antarctic ice core (Fig. 4a–b). The deglacial melting signal indicated by low benthic δ^{18}O values during Termination II (Risebrobakken et al., 2006; Bauch and Erlenkeuser, 2008) also ends, within age uncertainties, with the beginning of the North Atlantic benthic O-plateau (Fig. 4c). δ^{18}O values of the LIG benthic plateau are about 1 ‰ higher in the Norwegian Sea than in the North Atlantic (Fig. 4c). This is consistent with Norwegian Sea deep waters being colder by 3 to 4 °C than North Atlantic deep waters during interglacials (Labeyrie et al., 1987). Again, we tied the midpoint of the cooling transition at the end of the LIG (indicated by increasing percentages of *N. pachyderma* sinistral) to the enhanced cooling recorded in NGRIP δ^{18}O record (Fig. 4a–b). A simultaneous increase (within age uncertainties) in benthic δ^{18}O records from the Norwegian Sea and the North Atlantic after ∼120 ka (Fig. 4c) supports this tie-point. The maximum age uncertainty on records from the Norwegian Sea is estimated to be ±2.2 ka (1 σ) over the period 130–115 ka (Table 3).

3.2 Evidence for a global late LIG climatic optimum at high northern latitudes

3.2.1 Evolution of surface waters during the LIG

The evolution of northern and southern surface-water conditions is reported in Fig. 5. The Southern Ocean core record indicates the establishment of peak interglacial SSTs at 130 ka at high southern latitudes (Fig. 5b), i.e. immediately at the end of the deglacial warming recorded in southern subpolar waters during Termination II. In contrast, the SST reconstructions from subpolar regions show that peak interglacial SSTs occur at 125 ka in the Labrador Sea and the Norwegian Sea (Fig. 5d). In the North Atlantic at 55° N, the large deglacial surface-water warming associated with Termination II ends at 129 ka (Fig. 5b). It is followed by relatively stable SSTs during around 3.5 ka and an additional warming of 2 °C at 125.5 ka, which leads to maximal North Atlantic SST at 125 ka (Fig. 5b). We finally observe a gradual increase in surface-water temperature at mid-latitudes (42° N) in the North Atlantic during the LIG (Cortijo et al., 1999) (Fig. 5b). Therefore SST records from the Labrador Sea, Norwegian Sea and high-latitude North Atlantic indicate the establishment of optimal thermal conditions at 125 ka at high northern latitudes, i.e. 5 ka after the beginning of peak interglacial SSTs in the Southern Ocean.

We hence identify at the beginning of the LIG benthic O-plateau, an interval lasting three to four thousands years (period 129–125.5 ka, hereafter called "early LIG") characterized by: (1) peak interglacial conditions in the Southern Hemisphere, and (2) high northern latitude surface waters colder than in the later part of the benthic O-plateau (period 125–119 ka, hereafter called "late LIG"). The late establishment of oceanic thermal conditions that we document at high northern latitudes seems a consistent feature of the LIG climatic evolution in the Norwegian Sea (Rasmussen et al., 2003b; Bauch and Erlenkeuser, 2008; Bauch et al., 2011; Van Nieuwenhove et al., 2011). Our results suggest that the LIG delay in peak interglacial warmth is not restricted to the Norwegian Sea and extended to the Labrador Sea and high-latitude North Atlantic. The establishment of warm surface-water conditions at 125 ka in the North Atlantic (55° N) takes place in two phases. The high-amplitude (9° C) deglacial warming between 130.5 and 128.5 ka precedes a second warming of 2 °C at 125.5 ka leading to optimal thermal conditions at 125 ka (Fig. 5b). The relatively small amplitude of this additional warming probably explains why the LIG delay in peak interglacial warmth is not visible in lower-resolution records from the North Atlantic (Oppo et al., 2001; Rasmussen et al., 2003b; Kandiano et al., 2004; Bauch and Kandiano, 2007).

The late North Atlantic thermal optimum is associated with a delay in peak interglacial salinities in North Atlantic surface waters. Reconstructions of seawater δ^{18}O (Fig. 5c) show peak surface-water δ^{18}O values at around 122 ka at 42° N in the North Atlantic. At 55° N, high surface-water δ^{18}O values similar to Holocene values mark the

CPD
7, 3239–3286, 2011

beginning of the LIG at 129 ka (Fig. 5c). An additional increase in seawater δ^{18}O of 0.5 ‰ at around 125.5 ka however leads to the establishment of peak surface-water δ^{18}O values at 55° N at 125 ka only (Fig. 5c). North Atlantic surface waters are thus relatively fresher during the early LIG than during the late LIG (Fig. 5c). This feature is consistent with lower salinities recorded during the early LIG in the Norwegian Sea (Van Nieuwenhove and Bauch, 2008; Bauch et al., 2011).

Finally, IRD data indicate the persistence of iceberg melting until around 126 ka in the North Atlantic and in the Norwegian Sea (Fig. 5e). This result is consistent with persistent IRD documented after Termination II on the Vøring Plateau in the Norwegian Sea (Van Nieuwenhove and Bauch, 2008). The disappearance of iceberg melting at 126 ka coincides, within age uncertainties, with the latest estimates of the LIG sea level highstand registered by corals (Waelbroeck et al., 2008; Blanchon et al., 2009). Iceberg melting hence persists at high northern latitudes within the LIG benthic O-plateau recorded in North Atlantic and Southern Ocean cores (Fig. 5a). Available data do not allow us to assign the specific geographical origin of the icebergs. However, icebergs are probably released by the remnant melting of the Northern ice sheets (NIS), in particular the Eurasian Saalian ice sheet (Svendsen et al., 2004; Lambeck et al., 2006). Iceberg melting likely contributes to maintain the relatively colder and fresher surface-water conditions observed at high northern latitudes during the early LIG compared to the late LIG.

3.2.2 Evolution of deep waters during the LIG

These particular northern surface-water conditions during the early LIG have their counterpart at depth (Fig. 6). Benthic δ^{13}C data reveal variations in deep-water ventilation patterns between the early and late LIG (Fig. 6b). In the Southern Ocean, the increase in benthic δ^{13}C values by 0.8 ‰ during Termination II leads to benthic δ^{13}C values around −0.1 ‰ at the beginning of the LIG at 130.5 ka (Fig. 6b). Although these values are slightly lower than the ones recorded at the Southern Ocean site during the

Discussion Paper | Discussion Paper | Discussion Paper | Discussion Paper |

CPD

7, 3239–3286, 2011

Last Interglacial climate and ice sheet melting

A. Govin et al.

early Holocene (+0.2 ‰), they indicate the presence of already well-ventilated bottom waters in the deep Southern Ocean during the early LIG compared to the penultimate glacial period. The increase in benthic δ^{13}C values recorded during Termination II at different water depths in the North Atlantic lags by ~3 ka the benthic δ^{13}C increase in the Southern Ocean (Fig. 6b). This feature suggests a delay in the deglacial reorganization of North Atlantic deep waters during Termination II (Oppo et al., 1997).

Only the shallowest North Atlantic core indicates the presence of well-ventilated waters at 2000 m at the beginning of the LIG around 128 ka (Fig. 6b). During the interval 129–125.5 ka, this core exhibits δ^{13}C values of ~0.8 ‰, i.e. higher by ~0.4 ‰ than the two deepest North Atlantic sites (Fig. 6b). Such a strong δ^{13}C gradient between North Atlantic intermediate and deep waters during the early LIG is supported by further data from the North Atlantic (Keigwin et al., 1994; Oppo et al., 1997; Hodell et al., 2009). This δ^{13}C gradient reflects the persistent influence of bottom waters of southern origin in the deep North Atlantic during the early LIG (Oppo et al., 1997), i.e. the formation of a well-ventilated NADW that is less dense than during the late LIG. This feature is consistent with a weak North Atlantic deep-water circulation persistent at the beginning of the LIG on Gardar Drift (Iceland Basin) (Hodell et al., 2009). It is only during the late LIG, when the delivery of icebergs has ended and when northern surface waters are warm and saline (Fig. 5), that the deep ocean circulation becomes similar to the modern one. During that period, all North Atlantic cores between 2200 and 4100 m water depth exhibit high δ^{13}C values around 0.8 ‰ (Fig. 6b). These δ^{13}C values indicate the presence of the same water-mass, similar to the present-day high-ventilated NADW, between 2000 and 4000 m in the North Atlantic.

Our compilation of LIG data from the high northern and southern latitudes shows evidence for a persistent iceberg delivery at high northern latitudes during the early LIG. It is associated with relatively low salinity and temperature values in North Atlantic surface waters (Fig. 5), as well as a relatively weak ventilation of North Atlantic deep waters (Fig. 6) during the early LIG (129–125.5 ka) compared to the late LIG. The delay in peak interglacial warmth documented in the Norwegian Sea (Bauch and

Erlenkeuser, 2008; Bauch et al., 2011; Van Nieuwenhove et al., 2011) hence affects the Labrador Sea and high-latitude North Atlantic regions and has its counterpart at depth. Oceanic conditions at high northern latitudes are hence intermediate between glacial and full interglacial conditions at the beginning of the LIG. They are in contrast with the Southern Ocean climate evolution, which exhibits maximum interglacial warmth and well-ventilated bottom waters from the beginning of the LIG at ~130 ka.

4 Model-data comparison: possible climate processes responsible for the LIG climate evolution

Delays in peak warmth conditions between the northern and southern high latitudes, similar to what we observe at the beginning of the LIG, are attributed to "bipolar seesaw" mechanisms during the last glacial period (e.g. Blunier and Brook, 2001). During Termination II, rapid northern ice sheet melting however suppressed the imprint of "bipolar seesaw" signals (northern temperature reversal) in climate records from the penultimate deglaciation (Ruddiman et al., 1980; Carlson, 2008). Boreal summer insolation values of the LIG exceed the early Holocene maximum value during 7 ka at the beginning of the LIG (period 131–124 ka, Fig. 6c). In this section, we propose potential climate forcing and mechanisms responsible for the late LIG establishment of peak interglacial warmth and North Atlantic deep-water circulation. From the results of the model simulations, we investigate (1) to which extent high northern latitude climate solely responds to insolation variations during the LIG and (2) what the signature of a massive ice sheet melting would be during the early LIG.

4.1 Oceanic response to insolation changes during the LIG

We consider here the simulations performed with insolation as a sole forcing (Table 2): at 126 ka (high boreal summer insolation) and 122 ka (intermediate insolation values), in comparison to 115 ka (minimum in boreal summer insolation) (Fig. 6c). Figure 7

CPD
7, 3239–3286, 2011
Last Interglacial climate and ice sheet melting
A. Govin et al.

presents changes in surface and deep waters in the North Atlantic and Nordic Seas between these three time slices.

Northern high-latitude surface waters are warmer by 1.5 to 3 °C at 126 ka than at 122 ka, and by around 1 °C at 122 ka than at 115 ka (Fig. 7a). These temperature changes reflect the direct response of northern high-latitude climate to the boreal summer insolation, which gradually decreases between 126 and 115 ka (Fig. 6c). The high obliquity at 126 ka brings more direct solar radiation in high latitudes, thereby smoothing the temperature contrast between the tropics and the pole. As a consequence, a reduction in the total polar heat transport by the coupled ocean-atmosphere circulation is simulated between 126 and 122 ka (Fig. 7c). It mainly results from a reduction in the atmospheric heat transport reaching up to 0.25 PW (1 PW = 10^{15} W) at 20° N between 126 and 122 ka (Fig. 7c). Although only slightly affected by insolation changes, the poleward ocean heat transport remains higher at 126 ka compared to 122 ka (Fig. 7c). This increase is mainly due to changes in the North Atlantic sector (up to 0.10 PW). Therefore, higher North Atlantic SSTs at 126 ka compared to 122 ka reflects the increase in the Atlantic poleward heat transport. Figure 7d indicates that this increase in Atlantic heat transport at 126 ka is mainly due to a stronger Atlantic overturning between the equator and 40° N and a stronger subpolar gyre around 50° N (see Born et al., 2010).

Future climate simulations with increasing atmospheric carbon dioxide concentrations show that increased North Atlantic SSTs stratify the upper water, thereby limiting the deep convection that feeds the AMOC (Gregory et al., 2005). The model however simulates here a stronger AMOC at 126 ka than at 122 ka (Fig. 7b), due to the sinking of denser NADW (Fig. 7b). The reasons for a stronger AMOC at 126 ka compared to at 122 ka are twofold. (1) SST in late winter, when convection mostly occurs in the North Atlantic, is not different between the two periods, limiting the upper layer stabilizing effect. (2) A mechanism involves the export of Arctic sea ice towards the Nordic Seas where sea ice melts. In the warmer climate at 126 ka, the production of sea ice in the Arctic is reduced, so that the export of sea ice through Fram Strait is

CPD
7, 3239–3286, 2011

reduced by 0.04 Sv at 126 ka compared to 122 ka. This reduced export of sea ice from the Arctic to the Atlantic Ocean tends to decrease the sea surface salinity (SSS) in the Arctic at 126 ka compared to 122 ka. Furthermore less sea ice melts in the Nordic Seas, which increases the SSS in the Nordic Seas (not shown), sustains deep-water convection in the North Atlantic and a stronger AMOC at 126 ka compared to 122 ka. A similar mechanism has been proposed for simulations of future climate (Hu et al., 2004; Swingedouw et al., 2007a) and at the demise of the LIG (Born et al., 2010). In the study of the last glacial inception, Born et al. (2010) documented with the same climate model a weaker AMOC at 115 ka than at 126 ka due to this enhanced advection of Arctic sea ice into the North Atlantic. We observe here very little change in the Atlantic overturning (<0.5 Sv, $1\ \mathrm{Sv} = 10^6\ \mathrm{m}^3\ \mathrm{s}^{-1}$) between 122 ka and 115 ka (Fig. 7b). Similarly, changes in the Atlantic oceanic heat transport (in particular in the overturning component) remain low (<0.05 PW) between 122 ka and 115 ka (Fig. 7d), while the globally decreased atmospheric heat transport in the Northern Hemisphere account for the reduction in total heat transport (Fig. 7c). Therefore, most of the AMOC reduction identified between 126 and 115 ka during the last glacial inception (Born et al., 2010) occurs within the LIG between 126 and 122 ka. We attribute this major change in AMOC during the LIG to the increasing rate of insolation change (mainly linked to the obliquity change) between 126 and 122 ka, while it decreases between 122 and 115 ka (Fig. 6c).

In summary, the climate model simulates a warmer climate at high northern latitudes and more intense AMOC during the early LIG (126 ka) compared to the later LIG (122 ka) in response to insolation changes. These modeling results are in contradiction with proxy data, which indicate colder surface waters at high northern latitudes and a shallower NADW cell during the early LIG compared to the late LIG. Insolation variations are hence not the sole factors regulating the climate at high northern latitudes at the beginning of the LIG.

4.2 Additional impact of ice sheet melting on North Atlantic climate

To evaluate the contribution of a persistent ice sheet melting on the LIG climate at high northern latitudes, we consider in addition the simulation performed at 126 ka with interactive freshwater input ("126 ka meltwater").

When comparing the two simulations at 126 ka ("126 ka" and "126 ka meltwater", Fig. 8), we observe colder surface waters of up to 3 °C in the North Atlantic and the Nordic Seas (up to 65° N) when the meltwater is active at 126 ka (Fig. 8a). The warming observed at higher latitudes in the Norwegian Sea (Fig. 8a) is a common feature simulated in freshwater experiments by coupled ocean-atmosphere GCM (e.g. Stouffer et al., 2006, see discussion in Sect. 4.3.3 below). In addition, the model simulates a freshening of surface waters (not shown) at high northern latitudes, which is directly linked to the freshwater input. The supply of freshwater also stratifies the upper ocean and lowers the density of NADW (Fig. 8b). It results in a decrease in the strength of the AMOC by 6 Sv (Fig. 8b), which corresponds to a 50 % reduction of the AMOC intensity at 126 ka. The weakening of the AMOC in the "126 ka meltwater" simulation induces a strong reduction in the poleward heat transport by the Atlantic overturning (Fig. 8d). The resulting decrease in ocean heat transport (Fig. 8c) explains the cooling simulated in North Atlantic surface waters (Fig. 8a).

The climatic patterns described above at 126 ka correspond to classical North Atlantic climate responses computed in freshwater experiments by coupled models (e.g. Stouffer et al., 2006; Swingedouw et al., 2009). We also observe similar climate features simulated at high northern latitudes when considering the LIG climate evolution highlighted by the simulation at 126 ka with interactive freshwater input and the one at 122 ka. Surface waters in the North Atlantic (south of 60° N) are colder by up to 2 °C (Fig. 8a) and fresher (not shown) at 126 ka when the meltwater is active compared to at 122 ka. These characteristics are consistent with proxy-data SST and $\delta^{18}O_{sw}$ variations, which indicate colder and fresher conditions at high northern latitudes during the early LIG compared to the late LIG (Sect. 3.2.1). The simulated AMOC is also reduced by 4 Sv at 126 ka compared to 122 ka (Fig. 8b). The AMOC weakening is due to the reduction of NADW production in response to the surface freshwater input at 126 ka (Fig. 8b). The AMOC reduction simulated between 126 ka and 122 ka also results in a decrease in the poleward Atlantic heat transport (Fig. 8d), which explains the cooling of North Atlantic surface waters (Fig. 8a). This AMOC weakening is consistent with a shallow NADW cell indicated by North Atlantic proxy data at the beginning of the LIG (Sect. 3.2.2). The North Atlantic response computed by the model at 126 ka with interactive freshwater input compared to 122 ka shows a better agreement with the LIG climate evolution highlighted by marine sediment cores. These results show that the persistent melting of northern ice-sheet melting at the beginning of the LIG needs to be considered in addition to insolation variations, in order to reproduce the late establishment of peak interglacial conditions indicated by proxy data at high northern latitudes. Our model-data intercomparison however presents some limitations that we discuss in the next section.

4.3 Discussion on the limitations of the model-data comparison

4.3.1 Origin of the icebergs and melting water

In the model simulation, the meltwater input originates from the Greenland ice sheet, which is the only northern ice sheet represented in the model configuration. The freshwater flux computed is then redistributed in the Atlantic to the north of 40° N (Marti et al., 2010). The model simulations can hence represent the ocean and climate responses to the melting of unspecified northern ice sheets. Available data do not allow identifying the specific northern origin of ice-rafted detritus that are found in marine sediment cores from the North Atlantic and the Norwegian Sea at the beginning of the LIG (Fig. 5e). IRD are recorded at high northern latitudes at a time during the early LIG when North Atlantic benthic δ^{18}O values remain low and when benthic δ^{18}O variations smaller than 0.2 ‰ indicate sea level fluctuations smaller than 20 m (Fig. 5). This feature suggests that most glacial ice sheets have already melted away and that icebergs originate from the remnants of northern ice sheets. The Eurasian Saalian ice sheet, which extended during MIS 6 further south than during any subsequent glacial episode (e.g. Svendsen et al., 2004), constitutes a reasonable source for the melting icebergs. The influence of the melting Laurentide or Greenland ice sheets can however not be excluded.

4.3.2 Magnitude of the computed freshwater flux and North Atlantic response

The magnitude of the AMOC in the IPSL-CM4 model used here is known to be too low under preindustrial conditions compared to estimates based on observations (Swingedouw et al., 2007b). Nevertheless, the AMOC sensitivity to standard freshwater inputs (e.g. Stouffer et al., 2006) remains within the sensitivity of most coupled GCMs (Swingedouw et al., 2009).

The freshwater flux computed in response to the melting of the Greenland ice sheet under the strong insolation forcing at 126 ka is very large (0.17 Sv). It explains the strong reduction in the Atlantic overturning circulation (4 Sv, i.e. 38 % of the preindustrial simulation) observed between the simulations at 126 ka with interactive freshwater flux and at 122 ka (Fig. 8b). The large input of freshwater computed here is unrealistic for the LIG. For example, such a meltwater flux would imply the disappearance of the modern Greenland ice sheet (volume of 2.93×10^6 km^3, Bamber et al., 2001) in around 550 years. This value contradicts the reduction (not disappearance) of the Greenland ice sheet reconstructed for the LIG (e.g. Koerner, 1989; Otto-Bliesner et al., 2006). The simulation performed at 126 ka with the interactive freshwater flux should hence be considered as a maximum perturbation of the North Atlantic climate during the LIG induced by an extreme input of meltwater. Melting with such a magnitude could have only occurred on a very limited time scale. The climate conditions computed in the "126 ka meltwater" simulation are probably representative of climate conditions at the very beginning of the LIG (e.g. ~130–129 ka), when intense iceberg discharge took place at high northern latitudes. The "real" ocean and climate responses to insolation variations and meltwater input during the early LIG are likely to be intermediate between the two simulations at 126 ka, with and without the interactive freshwater input.

These discrepancies between model simulations and proxy data highlight here the critical need for including ice sheet models in coupled GCMs to improve the computation of freshwater fluxes and more realistically simulate the climate of the LIG.

4.3.3 Climatic response in the Norwegian Sea

Model results and proxy data disagree on the climatic response during the early LIG in the Norwegian Sea. Marine sediment cores record a late thermal optimum during the LIG, i.e. colder SST during the early LIG than the late LIG. The delay in the establishment of peak interglacial warmth indicated by marine records during the LIG appears to be a robust feature of the LIG climate evolution in the entire Norwegian Sea (Fronval and Jansen, 1997; Fronval et al., 1998; Rasmussen et al., 2003b; Bauch and Erlenkeuser, 2008; Bauch et al., 2011; Van Nieuwenhove et al., 2011). Although uncertainties on the chronologies of sediment cores from the Norwegian Sea remain relatively high for the LIG, independent age models of Norwegian Sea cores based on tephra layers support the late thermal optimum in the Nordic Seas (Wastegaard and Rasmussen, 2001; Rasmussen et al., 2003b).

In contrast, the IPSL-CM4 model simulates a warming of several degrees in the Norwegian Sea between the early LIG ("126 ka meltwater" simulation) and late LIG ("122 ka" simulation) (Fig. 8a). Given the large amount of freshwater redistributed at high northern latitudes in the model (see Sect. 4.3.2), the magnitude of this warming is probably overestimated in comparison to a potential "real" surface-water warming signal in the Norwegian Sea. This warming pattern, which is observed in response to freshwater input under different climate conditions, is a common feature of freshwater experiments in this model (Swingedouw et al., 2009). It is due to the adjustment of atmospheric dynamics in response to the initial global cooling. The changes in atmospheric dynamics increases the surface currents and the contribution of the gyre to the Atlantic heat transport north of 60° N (Fig. 8d). These two effects (wind and

CPD
7, 3239–3286, 2011

Last Interglacial climate and ice sheet melting

A. Govin et al.

ocean) reduce the sea ice cover along the eastern coast of Greenland, which leads to a warming in the Norwegian Sea (see Swingedouw et al., 2009 for further details). This warming pattern is not only a characteristic of the IPSL-CM4 model. Most atmosphere-ocean coupled models simulate this warming signal in the Nordic Seas in response to freshwater input (e.g. Stouffer et al., 2006; Saenko et al., 2007). Further studies on the reasons for such adjustments of the atmospheric circulation appear to be necessary to reconcile the LIG climate history seen by model simulations and proxy data in the Norwegian Sea.

5 Conclusions

Our compilation of proxy data for the LIG documents a delay in the establishment of peak interglacial conditions at high northern latitudes compared to high southern latitudes. We observe a persistent northern freshwater supply at the beginning of the LIG. It is associated with (1) relatively low salinity and temperature values in surface waters from the North Atlantic, Labrador and Norwegian Seas, and (2) a relatively weak ventilation of North Atlantic deep waters during the early LIG (129–125.5 ka) compared to the late LIG. These results indicate that the late thermal optimum documented in the Norwegian Sea (Bauch and Erlenkeuser, 2008; Bauch et al., 2011; Van Nieuwenhove et al., 2011) also takes place in the Labrador Sea and high-latitude North Atlantic regions. It also has its counterpart at depth, with a shallower North Atlantic deep water cell during the early LIG (Hodell et al., 2009). At the beginning of the LIG, oceanic conditions at high northern latitudes are hence intermediate between glacial and full interglacial conditions.

The comparison with model results indicates that the delay in peak interglacial conditions at high northern latitudes cannot be a direct response to insolation variations. In response to the sole insolation forcing, North Atlantic surface waters are warmer and more saline during the early LIG (126 ka) compared to the late LIG (122 ka). In that case, the Atlantic thermohaline circulation is also stronger at 126 ka than at 122 ka.

CPD
7, 3239–3286, 2011

We also show that most of this AMOC reduction within the LIG accounts for the AMOC decrease simulated during the last glacial inception (Born et al., 2010), probably in relationship to the increasing rate of insolation change between 126 and 122 ka. Therefore the modeled climate response to insolation variations is in contradiction to the LIG climate evolution indicated by proxy data. The model better reproduces the LIG climate history when the melting of northern ice sheets is considered during the early LIG (126 ka). North Atlantic surface waters are indeed colder and fresher, and the Atlantic meridional overturning weaker, at 126 ka with interactive freshwater flux compared to 122 ka. Insolation variations and persistent northern meltwater input hence need to be both considered in order to reproduce the late establishment of peak interglacial conditions during the LIG. This result emphasizes the sensitivity of North Atlantic climate to the melting of northern ice sheets in a warm climate and the necessity to consider ice-sheet melting in the simulations of warm climates. Finally, the model-data comparison reveals the limits of ocean-atmosphere coupled models to realistically simulate the magnitude of freshwater input and climatic responses. Our study hence highlights the critical need of developing ice sheet-climate coupled models to reliably simulate the evolution of warm past and future climates.

Acknowledgements. We would like to thank Gulay Isguder (LSCE) and Fabien Dewilde (LSCE) for increasing the resolution of respectively the SST and benthic isotopic records from core MD02-2488. Discussions with Dominique Raynaud and Didier Paillard helped to improve an early version of the manuscript. We also would like to thank the crew of the research vessel Marion-Dufresne and the French Paul Emile Victor Institute (IPEV) (especially Yvon Balut) for collecting most of the cores studied here. Funding of the cruises has been facilitated by IMAGES scientific collaborations. Part of this study has been performed within the framework of the French National Research Agency ANR PICC project. The research leading to these results has received funding from the European Union's Seventh Framework programme (FP7/2007-2013) under grant agreement no. 243908, "Past4Future. Climate change – Learning from the past climate".

The publication of this article is financed by CNRS-INSU.

References

Adkins, J. F., Boyle, E. A., Keigwin, L. D., and Cortijo, E.: Variability of the North Atlantic thermohaline circulation during the last interglacial period, Nature, 390, 154–156, 1997.

Andersson, C., Pausata, F. S. R., Jansen, E., Risebrobakken, B., and Telford, R. J.: Holocene trends in the foraminifer record from the Norwegian Sea and the North Atlantic Ocean, Clim. Past, 6, 179–193, doi:10.5194/cp-6-179-2010, 2010.

Bamber, J. L., Layberry, R. L., and Gogineni, S. P.: A new ice thickness and bed data set for the Greenland ice sheet 1. Measurement, data reduction, and errors, J. Geophys. Res., 106, 33773–33780, doi:10.1029/2001jd900054, 2001.

Bard, E., Arnold, M., and Duplessy, J. C.: Reconciling the sea level record of the last deglaciation with the $\delta^{18}O$ spectra from deep sea cores, in: Radiocarbon dating: recent applications and future potential, edited by: Lowe, J. J., Quaternary Proceedings, Quaternary Research Association, Cambridge, 67-73, 1991.

Bauch, H. A. and Kandiano, E. S.: Evidence for early warming and cooling in North Atlantic surface waters during the last interglacial, Paleoceanography, 22, PA1201, doi:10.1029/2005PA001252, 2007.

Bauch, H. A. and Erlenkeuser, H.: A “critical” climatic evaluation of last interglacial (MIS 5e) records from the Norwegian Sea, Polar Res., 27, 135–151, 2008.

Bauch, H. A., Kandiano, E. S., Helmke, J., Andersen, N., Rosell-Mele, A., and Erlenkeuser, H.: Climatic bisection of the last interglacial warm period in the Polar North Atlantic, Quaternary Sci. Rev., 30, 1813–1818, doi:10.1016/j.quascirev.2011.05.012, 2011.

Berger, A. and Loutre, M. F.: Insolation values for the climate of the last 10 million years, Quaternary Sci. Rev., 10, 297–317, 1991.

Berger, A. L.: Long-Term Variations of Daily Insolation and Quaternary Climatic Changes, J. Atmos. Sci., 35, 2362–2367, 1978.
Birks, C. J. A. and Koç, N.: A high-resolution diatom record of late-Quaternary sea-surface temperatures and oceanographic conditions from the eastern Norwegian Sea, Boreas, 31, 323–344, doi:10.1111/j.1502-3885.2002.tb01077.x, 2002.
Blanchon, P., Eisenhauer, A., Fietzke, J., and Liebetrau, V.: Rapid sea-level rise and reef back-stepping at the close of the last interglacial highstand, Nature, 458, 881–884, 2009.
Blunier, T. and Brook, E. J.: Timing of millenial-scale climate change in Antarctica and Greenland during the Last Glacial Period, Science, 291, 109–112, 2001.
Bond, G. C., Broecker, W., Johnsen, S., McManus, J., Labeyrie, L., Jouzel, J., and Bonani, G.: Correlations between climate records from the North Atlantic sediments and Greenland Ice, Nature, 365, 143–147, 1993.
Born, A., Nisancioglu, K., and Braconnot, P.: Sea ice induced changes in ocean circulation during the Eemian, Clim. Dynam., 35, 1361–1371, doi:10.1007/s00382-009-0709-2, 2010.
Braconnot, P., Marzin, C., Grégoire, L., Mosquet, E., and Marti, O.: Monsoon response to changes in Earth's orbital parameters: comparisons between simulations of the Eemian and of the Holocene, Clim. Past, 4, 281–294, doi:10.5194/cp-4-281-2008, 2008.
Calvo, E., Grimalt, J., and Jansen, E.: High resolution U37K sea surface temperature reconstruction in the Norwegian Sea during the Holocene, Quaternary Sci. Rev., 21, 1385–1394, doi:10.1016/S0277-3791(01)00096-8, 2002.
Calvo, E., Pelejero, C., de Deckker, P., and Logan, G. A.: Antarctic deglacial pattern in a 30 kyr record of sea surface temperature offshore South Australia, Geophys. Res. Lett, 34, L13707, doi:10.1029/2007GL029937, 2007.
Cape Last Interglacial Project members: Last Interglacial Arctic warmth confirms polar amplification of climate change, Quaternary Sci. Rev., 25, 1383–1400, 2006.
Capron, E., Landais, A., Lemieux-Dudon, B., Schilt, A., Masson-Delmotte, V., Buiron, D., Chappellaz, J., Dahl-Jensen, D., Johnsen, S., Leuenberger, M., Loulergue, L., and Oerter, H.: Synchronising EDML and NorthGRIP ice cores using δ^{18}O of atmospheric oxygen (δ^{18}Oatm) and CH_4 measurements over MIS5 (80–123 kyr), Quaternary Sci. Rev., 29, 222–234, doi:10.1016/j.quascirev.2009.07.014, 2010.
Carlson, A. E.: Why there was not a Younger Dryas-like event during the Penultimate Deglaciation, Quaternary Sci. Rev., 27, 882–887, 2008.

CPD
7, 3239–3286, 2011

Chapman, M. R. and Shackleton, N. J.: Millennial-scale fluctuations in North Atlantic heat flux during the last 150,000 years, Earth Planet. Sc. Lett., 159, 57–70, 1998.
Clark, P. U. and Huybers, P.: Global change: Interglacial and future sea level, Nature, 462, 856–857, doi:10.1038/462856a, 2009.
Cortijo, E., Duplessy, J. C., Labeyrie, L., Leclaire, H., Duprat, J., and van Weering, T. C. E.: Eemian cooling in the Norwegian Sea and North Atlantic ocean preceding continental ice-sheet growth, Nature, 372, 446–449, 1994.
Cortijo, E., Lehman, S., Keigwin, L., Chapman, M., Paillard, D., and Labeyrie, L.: Changes in meridional temperature and salinity gradients in the North Atlantic Ocean (30–72° N) during the last interglacial period, Paleoceanography, 14, 23–33, 1999.
Cutler, K. B., Edwards, R. L., Taylor, F. W., Cheng, H., Adkins, J., Gallups, C. D., Cutler, P. M., Burr, G. S., and Bloom, A. L.: Rapid sea-level fall and deep-ocean temperature change since the last interglacial period, Earth Planet. Sc. Lett., 206, 253–271, 2003.
Denton, G. H., Anderson, R. F., Toggweiler, J. R., Edwards, R. L., Schaefer, J. M., and Putnam, A. E.: The Last Glacial Termination, Science, 328, 1652–1656, doi:10.1126/science.1184119, 2010.
Desprat, S., Sanchez Goni, M. F., Naughton, F., Turon, J.-L., Duprat, J., Malaizé, B., Cortijo, E., and Peypouquet, J.-P.: Climate variability of the last five isotopic interglacials: direct land-sea-ice correlation from the multiproxy analysis of North-Western Iberian margin deep-sea cores, in: The Climate of Past Interglacials, edited by: Sirocko, F., Claussen, M., Sanchez Goni, M. F., and Litt, T., Developments in Quaternary Science, Vol. 7, Elsevier, Amsterdam, 375–386, 2007.
Dokken, T. and Jansen, E.: Rapid changes in the mechanism of ocean convection during the last glacial period, Nature, 401, 458–461, 1999.
Duplessy, J. C., Labeyrie, L., Juillet-Leclerc, A., Maitre, F., Duprat, J., and Sarnthein, M.: Surface salinity reconstruction of the North Atlantic Ocean during the last glacial maximum, Oceanol. Acta, 14, 311–324, 1991.
EPICA Community members: Eight glacial cycles from an Antarctic ice core, Nature, 429, 623–628, 2004.
EPICA Community members: One-to-one coupling of glacial climate variability in Greenland and Antarctica, Nature, 444, 195–198, 2006.

Discussion Paper | Discussion Paper | Discussion Paper | Discussion Paper |

CPD
7, 3239–3286, 2011

Last Interglacial climate and ice sheet melting

A. Govin et al.

Fronval, T. and Jansen, E.: Eemian and Early Weichselian (140–60 ka) Paleoceanography and Paleoclimate in the Nordic Seas With Comparisons to Holocene Conditions, Paleoceanography, 12, 443–462, doi:10.1029/97pa00322, 1997.
Fronval, T., Jansen, E., Haflidason, H., and Sejrup, H. P.: Variability in surface and deep water conditions in the Nordic Seas during the last interglacial period, Quaternary Sci. Rev., 17, 963–985, 1998.
Ganopolski, A. and Roche, D. M.: On the nature of lead-lag relationships during glacial-interglacial climate transitions, Quaternary Sci. Rev., 28, 3361–3378, doi:10.1016/j.quascire.2009.09.019, 2009.
Govin, A., Michel, E., Labeyrie, L., Waelbroeck, C., Dewilde, F., and Jansen, E.: Evidence for northward expansion of Antarctic Bottom Water mass in the Southern Ocean during the last glacial inception, Paleoceanography, 24, PA1202, doi:10.1029/2008PA001603, 2009.
Gregory, J. M., Stouffer, K. W. D., R, J., Weaver, A. J., Driesschaert, E., Eby, M., Fichefet, T., Hasumi, H., Hu, A., Jungclaus, J. H., Kamenkovich, I. V., Levermann, A., Montoya, M., Murakami, S., Nawrath, S., Oka, A., Sokolov, A. P., and Thorpe, R. B.: A model intercomparison of changes in the Atlantic thermohaline circulation in response to increasing atmospheric CO_2 concentration, Geophysical Res. Lett., 32, L12703, doi:10.1029/2005GL023209, 2005.
Hald, M., Andersson, C., Ebbesen, H., Jansen, E., Klitgaard-Kristensen, D., Risebrobakken, B., Salomonsen, G. R., Sarnthein, M., Sejrup, H. P., and Telford, R. J.: Variations in temperature and extent of Atlantic Water in the northern North Atlantic during the Holocene, Quaternary Sci. Rev., 26, 3423–3440, doi:10.1016/j.quascirev.2007.10.005, 2007.
Hodell, D. A., Minth, E. K., Curtis, J. H., McCave, I. N., Hall, I. R., Channell, J. E. T., and Xuan, C.: Surface and deep-water hydrography on Gardar Drift (Iceland Basin) during the last interglacial period, Earth Planet. Sc. Lett., 288, 10–19, doi:10.1016/j.epsl.2009.08.040, 2009.
Hu, A., Meehl, G., Washington, W., and Dai, A.: Response of the Atlantic thermohaline circulation to increased atmospheric CO_2 in a coupled model, J. Climate, 17, 4267–4279, 2004.
Jansen, E., Overpeck, J. T., Briffa, K. R., Duplessy, J. C., Joos, F., Masson-Delmotte, V., Olago, D., Otto-Bliesner, B., Peltier, W. R., Rahmstorf, S., Ramesh, R., Raynaud, D., Rind, D., Solomina, O., Villalba, R., and Zhang, D.: Palaeoclimate, in: Climate Change 2007: The Physical Science Basis, Contribution of Working Group I to the Four Assessment Report of the Intergovernmental Panel on Climate Change, edited by: Solomon, S., Qin, D., Manning, M., Chen, Z., Marquis, M., Averyt, K. B., Tignor, M., and Miller, H. L., Cambridge University

Press, Cambridge, UK and New York, NY, USA, 2007.

Jouzel, J., Masson-Delmotte, V., Cattani, O., Dreyfus, G., Falourd, S., Hoffmann, G., Minster, B., Nouet, J., Barnola, J. M., Chappellaz, J., Fischer, H., Gallet, J. C., Johnsen, S., Leuenberger, M., Loulergue, L., Luethi, D., Oerter, H., Parrenin, F., Raisbeck, G., Raynaud, D., Schilt, A., Schwander, J., Selmo, E., Souchez, R., Spahni, R., Stauffer, B., Steffensen, J. P., Stenni, B., Stocker, T. F., Tison, J. L., Werner, M., and Wolff, E. W.: Orbital and Millennial Antarctic Climate Variability over the Past 800,000 Years, Science, 317, 793–796, doi:10.1126/science.1141038, 2007.

Kandiano, E. S., Bauch, H. A., and Müller, A.: Sea Surface temperature variability in the North Atlantic during the last two glacial-interglacial cycles: comparison of faunal, oxygen isotopic, and Mg/Ca-derived records, Palaeogeogr. Palaeocl., 204, 145–164, 2004.

Keigwin, L. D., Curry, W. B., Lehman, S. J., and Johnsen, S.: The role of the deep ocean in North Atlantic climate change between 70 and 130 kyr ago, Nature, 371, 323–326, 1994.

Kelly, M. J., Edwards, R. L., Cheng, H., Yuan, D., Cai, Y., Zhang, M., Lin, Y., and An, Z.: High resolution characterization of the Asian Monsoon between 146,000 and 99,000-years B.P. from Dongge Cave, China and global correlation of events surrounding Termination II, Palaeogeogr. Palaeocl., 236, 20–38, doi:10.1016/j.palaeo.2005.11.042, 2006.

Koerner, R. M.: Ice Core Evidence for Extensive Melting of the Greenland Ice Sheet in the Last Interglacial, Science, 244, 964–968, doi:10.1126/science.244.4907.964, 1989.

Kopp, R. E., Simons, F. J., Mitrovica, J. X., Maloof, A. C., and Oppenheimer, M.: Probabilistic assessment of sea level during the last interglacial stage, Nature, 462, 863–867, doi:10.1038/nature08686, 2009.

Kucera, M., Weinelt, M., Kiefer, T., Pflaumann, U., Hayes, A., Chen, M. T., Mix, A. C., Barrows, T. T., Cortijo, E., Duprat, J., Juggins, S., and Waelbroeck, C.: Reconstruction of sea-surface temperatures from assemblages of planktonic foraminifera: multi-technique approach based on geographically constrained calibration data sets and its application to glacial Atlantic and Pacific Oceans, Quaternary Sci. Rev., 24, 951–998, 2005.

Kukla, G., McManus, J. F., Rousseau, D. D., and Chuine, I.: How long and how stable was the last interglacial?, Quaternary Sci. Rev., 16, 605–612, 1997.

Kukla, G. J., Bender, M. L., de Beaulieu, J. L., Bond, G. C., Broecker, W., Cleveringa, P., Gavin, J. E., Herbert, T. D., Imbrie, J., Jouzel, J., Keigwin, L. D., Knudsen, K. L., McManus, J. F., Merkt, J., Muhs, D. R., Müller, H., Poore, R. Z., Porter, S. C., Seret, G., Shackleton, N. J., Turner, C., Tzedakis, P. C., and Winograd, I. J.: Last interglacial climates, Quaternary Res.,

58, 2–13, 2002.
Labeyrie, L., Duplessy, J. C., and Blanc, P. L.: Variations in mode of formation and temperature of oceanic deep waters over the past 125,000 years, Nature, 327, 477–482, 1987.
Labeyrie, L., Leclaire, H., Waelbroeck, C., Cortijo, E., Duplessy, J. C., Vidal, L., Elliot, M., and Le Coat, B.: Temporal variability of the surface and deep waters of the North West Atlantic Ocean at orbital and millenial scales, Geophys. Monogr., 112, 77–98, 1999.
Labeyrie, L., Waelbroeck, C., Cortijo, E., Michel, E., and Duplessy, J. C.: Changes in deep water hydrology during the last deglaciation, C. R. Geosci., 337, 919–927, 2005.
Lambeck, K., Purcell, A., Funder, S., Kjær, K. H., Larsen, E., and Moller, P. E. R.: Constraints on the Late Saalian to early Middle Weichselian ice sheet of Eurasia from field data and rebound modelling, Boreas, 35, 539–575, doi:10.1080/03009480600781875, 2006.
Loulergue, L., Parrenin, F., Blunier, T., Barnola, J.-M., Spahni, R., Schilt, A., Raisbeck, G., and Chappellaz, J.: New constraints on the gas age-ice age difference along the EPICA ice cores, 0-50 kyr, Clim. Past, 3, 527–540, doi:10.5194/cp-3-527-2007, 2007.
Loulergue, L., Schilt, A., Spahni, R., Masson-Delmotte, V., Blunier, T., Lemieux, B., Barnola, J. M., Raynaud, D., Stocker, T. F., and Chappellaz, J.: Orbital and millennial-scale features of atmospheric CH_4 over the past 800,000 years, Nature, 453, 383–386, 2008.
Marti, O., Braconnot, P., Dufresne, J. L., Bellier, J., Benshila, R., Bony, S., Brockmann, P., Cadule, P., Caubel, A., Codron, F., de Noblet, N., Denvil, S., Fairhead, L., Fichefet, T., Foujols, M. A., Friedlingstein, P., Goosse, H., Grandpeix, J. Y., Guilyardi, E., Hourdin, F., Idelkadi, A., Kageyama, M., Krinner, G., Lévy, C., Madec, G., Mignot, J., Musat, I., Swingedouw, D., and Talandier, C.: Key features of the IPSL ocean atmosphere model and its sensitivity to atmospheric resolution, Clim. Dynam., 34, 1–26, doi:10.1007/s00382-009-0640-6, 2010.
McManus, J. F., Oppo, D. W., and Cullen, J.: A 0.5-million-year record of millenial-scale climate variability in the North Atlantic, Science, 283, 971–975, 1999.
Meehl, G., Stocker, T. F., Collins, W. D., Friedlingstein, P., Gaye, A. T., Gregory, J. M., Kitoh, A., Knutti, R., Murphy, J. M., Noda, A., Raper, S. C. B., Watterson, I. G., Weaver, A. J., and Zhao, Z.-C.: Global Climate Projections, in: Climate change 2007: The Physical Science Basis, Contribution of Working Group I to the Fourth Assessment Report of the Intergovernmental Panel on Climate Change, edited by: Solomon, S., Qin, D., Manning, M., Chen, Z., Marquis, M., Averyt, K. B., Tignor, M., and Miller, H. L., Cambridge University Press, Cambridge, UK and New York, NY, USA, 2007.

CPD
7, 3239–3286, 2011

North Greenland Ice Core Project members: High-resolution climate record of Northern Hemisphere climate extending into the last interglacial period, Nature, 431, 147–151, 2004.
Oppo, D. W., Horowitz, M., and Lehman, S. J.: Marine core evidence for reduced deep water production during Termination II followed by a relatively stable substage 5e (Eemian), Paleoceanography, 12, 51–63, 1997.
Oppo, D. W., Keigwin, L. D., McManus, J. F., and Cullen, J. L.: Persistent suborbital climate variability in marine isotope stage 5 and Termination II, Paleoceanography, 16, 280–292, 2001.
Oppo, D. W., McManus, J. F., and Cullen, J.: Evolution and demise of the last interglacial warmth in the subpolar North Atlantic, Quaternary Sci. Rev., 25, 3268–3277, 2006.
Otto-Bliesner, B. L., Marshall, S. J., Overpeck, J. T., Miller, G. H., Hu, A., and members, C. L. I. P.: Simulating arctic climate warmth and icefield retreat in the Last Interglacial, Science, 311, 1751–1753, 2006.
Paillard, D., Labeyrie, L., and Yiou, P.: Macintosh program performs time-series analyses, Eos Trans. AGU, 77, 39, doi:10.1029/96EO00259, 1996.
Parrenin, F., Barnola, J.-M., Beer, J., Blunier, T., Castellano, E., Chappellaz, J., Dreyfus, G., Fischer, H., Fujita, S., Jouzel, J., Kawamura, K., Lemieux-Dudon, B., Loulergue, L., Masson-Delmotte, V., Narcisi, B., Petit, J.-R., Raisbeck, G., Raynaud, D., Ruth, U., Schwander, J., Severi, M., Spahni, R., Steffensen, J. P., Svensson, A., Udisti, R., Waelbroeck, C., and Wolff, E.: The EDC3 chronology for the EPICA Dome C ice core, Clim. Past, 3, 485–497, doi:10.5194/cp-3-485-2007, 2007.
Rasmussen, T. L., Oppo, D. W., Thomsen, E., and Lehman, S. J.: Deep sea records from the southeast Labrador Sea: ocean circulation changes and ice-rafting events during the last 160,000 years, Paleoceanography, 18, 1018, doi:10.1029/2001PA000736, 2003a.
Rasmussen, T. L., Thomsen, E., Kuijpers, A., and Wastegård, S.: Late warming and early cooling of the sea surface in the Nordic seas during MIS 5e (Eemian Interglacial), Quaternary Sci. Rev., 22, 809–821, 2003b.
Risebrobakken, B., Dokken, T., and Jansen, E.: Extent and variability of the Meridional Atlantic Circulation in the Eastern Nordic Seas during Marine Isotope Stage 5 and its influence on the inception of the last Glacial, in: The Nordic Seas: an integrated perspective, edited by: Drange, H., Dokken, T., Furevik, T., Gerdes, R., and Berger, W. H., AGU Geophys. Monogr., 323–339, 2005.

CPD
7, 3239–3286, 2011

Last Interglacial climate and ice sheet melting

A. Govin et al.

Risebrobakken, B., Balbon, E., Dokken, T., Jansen, E., Kissel, C., Labeyrie, L., Richter, T., and Senneset, L.: The penultimate deglaciation: high-resolution paleoceanographic evidence from a north-south transect along the eastern Nordic Seas, Earth Planet. Sc. Lett., 241, 505–516, 2006.

Risebrobakken, B., Dokken, T., Smedsrud, L. H., Andersson, C., Jansen, E., Moros, M., and Ivanova, E. V.: Early Holocene temperature variability in the Nordic Seas: The role of oceanic heat advection versus changes in orbital forcing, Paleoceanography, doi:10.1029/2011PA002117, in press, 2011.

Rohling, E. J., Grant, K., Hemleben, C., Siddall, M., Hoogakker, B. A. A., Bolshaw, M., and Kucera, M.: High rates of sea-level rise during the last interglacial period, Nat. Geosci., 1, 38–42, doi:10.1038/ngeo.2007.28, 2008.

Ruddiman, W. F., Molfino, B., Esmay, A., and Pokras, E.: Evidence bearing on the mechanism of rapid deglaciation, Climatic Change, 3, 65–87, 1980.

Ruth, U., Barnola, J.-M., Beer, J., Bigler, M., Blunier, T., Castellano, E., Fischer, H., Fundel, F., Huybrechts, P., Kaufmann, P., Kipfstuhl, S., Lambrecht, A., Morganti, A., Oerter, H., Parrenin, F., Rybak, O., Severi, M., Udisti, R., Wilhelms, F., and Wolff, E.: "EDML1": a chronology for the EPICA deep ice core from Dronning Maud Land, Antarctica, over the last 150 000 years, Clim. Past, 3, 475–484, doi:10.5194/cp-3-475-2007, 2007.

Saenko, O. A., Weaver, A. J., Robitaille, D. Y., and Flato, G. M.: Warming of the subpolar Atlantic triggered by freshwater discharge at the continental boundary, Geophys. Res. Lett., 34, 15604, doi:10.1029/2007GL030674, 2007.

Sarnthein, M. and Tiedemann, R.: Younger Dryas-Style Cooling Events at Glacial Terminations I–VI at ODP Site 658: Associated benthic δ^{13}C anomalies constrain meltwater hypothesis, Paleoceanography, 5, 1041–1055, 1990.

Severinghaus, J. P., Sowers, T., Brook, E. J., Alley, R. B., and Bender, M. L.: Timing of abrupt climate change at the end of the Younger Dryas interval from thermally fractionated gases in polar ice, Nature, 391, 141–146, 1998.

Shackleton, N. J.: The last interglacial in the marine and terrestrial records, P. Roy. Soc. Lond. B, 174, 135–154, 1969.

Shackleton, N. J.: Attainment of isotopic equilibrium between ocean water and the benthonic foraminifera genus Uvigerina: isotopic changes in the ocean during the last glacial, Colloques internationaux du CNRS, 219, 1974.

Shackleton, N. J., Hall, M. A., and Vincent, E.: Phase relationships between millenial-scale events 64,000–24,000 years ago, Paleoceanography, 15, 565–569, 2000.
Shackleton, N. J., Chapman, M. R., Sanchez-Goni, M. F., Pailler, D., and Lancelot, Y.: The classic Marine Isotope Substage 5e, Quaternary Res., 58, 14–16, 2002.
Siddall, M., Rohling, E. J., Almogi-Labin, A., Hemleben, C., Meischner, D., Schmelzer, I., and Smeed, D. A.: Sea-level fluctuations during the last glacial cycle, Nature, 423, 853–858, doi:10.1038/nature01690, 2003.
Skinner, L. C. and Shackleton, N. J.: An Atlantic lead over Pacific deep-water change across Termination I: implications for the application of the marine isotope stage stratigraphy, Quaternary Sci. Rev., 24, 571–580, 2005.
Skinner, L. C., Fallon, S., Waelbroeck, C., Michel, E., and Barker, S.: Ventilation of the Deep Southern Ocean and Deglacial CO_2 Rise, Science, 328, 1147–1151, doi:10.1126/science.1183627, 2010.
Smith, D. E., Harrison, S., Firth, C. R., and Jordan, J. T.: The early Holocene sea level rise, Quaternary Sci. Rev., 30, 1846–1860, doi:10.1016/j.quascirev.2011.04.019, 2011.
Stenni, B., Buiron, D., Frezzotti, M., Albani, S., Barbante, C., Bard, E., Barnola, J. M., Baroni, M., Baumgartner, M., Bonazza, M., Capron, E., Castellano, E., Chappellaz, J., Delmonte, B., Falourd, S., Genoni, L., Iacumin, P., Jouzel, J., Kipfstuhl, S., Landais, A., Lemieux-Dudon, B., Maggi, V., Masson-Delmotte, V., Mazzola, C., Minster, B., Montagnat, M., Mulvaney, R., Narcisi, B., Oerter, H., Parrenin, F., Petit, J. R., Ritz, C., Scarchilli, C., Schilt, A., Schupbach, S., Schwander, J., Selmo, E., Severi, M., Stocker, T. F., and Udisti, R.: Expression of the bipolar see-saw in Antarctic climate records during the last deglaciation, Nat. Geosci., 4, 46–49, doi:10.1038/ngeo1026, 2011.
Stouffer, R. J., Yin, J., Gregory, J. M., Dixon, K. W., Spelman, M. J., Hurlin, W., Weaver, A. J., Eby, M., Flato, G. M., and Hasumi, H.: Investigating the Causes of the Response of the Thermohaline Circulation to Past and Future Climate Changes, J. Climate, 19, 1365–1387, 2006.
Svendsen, J. I., Alexanderson, H., Astakhov, V. I., Demidov, I., Dowdeswell, J. A., Funder, S., Gataullin, V., Henriksen, M., Hjort, C., Houmark-Nielsen, M., Hubberten, H. W., Ingolfsson, O., Jakobsson, M., Kjær, K. H., Larsen, E., Lokrantz, H., Lunkka, J. P., Lysaa, A., Mangerud, J., Matiouchkov, A., Murray, A., Möller, P., Niessen, F., Nikolskaya, O., Polyak, L., Saarnisto, M., Siegert, C., Siegert, M. J., Spielhagen, R. F., and Stein, R.: Late Quaternary ice sheet history of northern Eurasia, Quaternary Sci. Rev., 23, 1229–1271,

doi:10.1016/j.quascirev.2003.12.008, 2004.
Swingedouw, D., Braconnot, P., Delecluse, P., Guilyardi, E., and Marti, O.: Quantifying the AMOC feedbacks during a $2 \times CO_2$ stabilization experiment with land-ice melting, Clim. Dynam., 29, 521-534, 2007a.
Swingedouw, D., Braconnot, P., Delecluse, P., Guilyardi, E., and Marti, O.: The impact of global freshwater forcing on the thermohaline circulation: adjustment of North Atlantic convection sites in a CGCM, Clim. Dynam., 28, 291–305, 2007b.
Swingedouw, D., Mignot, J., Braconnot, P., Mosquet, E., Kageyama, M., and Alkama, R.: Impact of Freshwater Release in the North Atlantic under Different Climate Conditions in an OAGCM, J. Climate, 22, 6377–6403, 2009.
Thompson, W. G. and Goldstein, S. L.: A radiometric calibration of the SPECMAP timescale, Quaternary Sci. Rev., 25, 3207–3215, doi:10.1016/j.quascirev.2006.02.007, 2006.
Van Nieuwenhove, N. and Bauch, H. A.: Last interglacial (MIS 5e) surface water conditions at the Vøring Plateau (Norwegian Sea), based on dinoflagellate cysts, Polar Res., 27, 175–186, doi:10.1111/j.1751-8369.2008.00062.x, 2008.
Van Nieuwenhove, N., Bauch, H. A., Eynaud, F., Kandiano, E., Cortijo, E., and Turon, J.-L.: Evidence for delayed poleward expansion of North Atlantic surface waters during the last interglacial (MIS 5e), Quaternary Sci. Rev., 30, 934–946, doi:10.1016/j.quascirev.2011.01.013, 2011.
Waelbroeck, C., Labeyrie, L., Michel, E., Duplessy, J. C., McManus, J. F., Lambeck, K., Balbon, E., and Labracherie, M.: Sea-level and deep water temperature changes derived from benthic foraminifera isotopic records, Quaternary Sci. Rev., 21, 295–305, 2002.
Waelbroeck, C., Levi, C., Duplessy, J. C., Labeyrie, L., Michel, E., Cortijo, E., Bassinot, F., and Guichard, F.: Distant origin of circulation changes in the Indian Ocean during the last deglaciation, Earth Planet. Sc. Lett., 243, 244–251, 2006.
Waelbroeck, C., Frank, N., Jouzel, J., Parrenin, F., Masson-Delmotte, V., and Genty, D.: Transferring radiometric dating of the last interglacial sea level high stand to marine and ice core records, Earth Planet. Sc. Lett., 265, 183–194, 2008.
Waelbroeck, C., Skinner, L. C., Labeyrie, L., Duplessy, J. C., Michel, E., Vazquez Riveiros, N., Gherardi, J. M., and Dewilde, F.: The timing of deglacial circulation changes in the Atlantic, Paleoceanography, 26, PA3213, doi:10.1029/2010pa002007, 2011.

Wastegaard, S. and Rasmussen, T. L.: New tephra horizons from Oxygen Isotope Stage 5 in the North Atlantic: correlation potential for terrestrial, marine and ice-core archives, Quaternary Sci. Rev., 20, 1587–1593, doi:10.1016/S0277-3791(01)00055-5, 2001.
Weldeab, S., Lea, D. W., Schneider, R. R., and Andersen, N.: 155,000 Years of West African Monsoon and Ocean Thermal Evolution, Science, 316, 1303–1307, doi:10.1126/science.1140461, 2007.

CPD
7, 3239–3286, 2011

Table 1. Cores considered in this study (the location of cores from the North Atlantic, Labrador and Norwegian Seas is shown in Fig. 7).

Ocean	Core	Latitude	Longitude	Depth	Reference
Norwegian Sea	MD95-2010	66.68° N	4.57° E	1226 m	Risebrobakken et al. (2005, 2006)
Labrador Sea	EW9302-JPC2	48.80° N	45.09° W	1251 m	Rasmussen et al. (2003b)
North Atlantic	ODP 980	55.49° N	14.70° W	2168 m	McManus et al. (1999); Oppo et al. (2006)
	CH69-K09	41.76° N	47.35° W	4100 m	Cortijo et al. (1999); Labeyrie et al. (1999)
	MD95-2042	37.80° N	10.17° W	3146 m	Shackleton et al. (2000, 2002)
Southern Ocean	MD02-2488	46.47° S	88.02° E	3420 m	Govin et al. (2009)

CPD
7, 3239–3286, 2011

CPD
7, 3239–3286, 2011

Table 2. Model simulations performed with the IPSL-CM4 coupled climate model considered in this study. The simulations are forced with the modern ice sheet configuration and pre-industrial greenhouse gas concentrations.

Name of simulation	Forcing	Reference
126 ka	Insolation values at 126 ka[1]	Braconnot et al. (2008)
122 ka	Insolation values at 122 ka[1,2]	Braconnot et al. (2008)
115 ka	Insolation values at 115 ka[1]	Braconnot et al. (2008)
126 ka meltwater	Insolation values at 126 ka[1] Interactive northern meltwater input (0.17 Sv)	Swingedouw et al. (2007a, 2009)

[1] Insolation values from Berger (1978).

[2] The simulation at 122 ka contains a small input of freshwater (0.03 Sv), which has a very limited impact on deep-water formation.

Table 3. Tie-points and associated age uncertainties (1 σ, in years) for each sediment core. The total age uncertainty (in bold) is derived from the quadratic sum of individual uncertainties[a].

Core	Depth (cm)	EDC3 age (ka)	Rational	Resolution of correlated record (y)	Resolution of reference record (y)	Matching uncertainty (y)	Uncertainty on the transfer of NGRIP on EDC3 time scale[b] (y)	Uncertainty on the gas-ice age difference of EDC[c] (y)	Total age uncertainty on EDC3 time scale (y)
Southern Ocean									
MD02-2488	2346.1	108.6	Temperature minimum between D/O 24 and D/O 25	240	73	800			**840**
	2431.3	111.9	Temperature minimum preceding D/O 25	150	70	800			**820**
	2494.3	116.8	Midpoint of temperature decrease	210	58	1200			**1300**
	2522.4	121.4	Beginning of temperature decrease	400	47	1200			**1300**
	2549.0	128.8	Temperature maxima	560	32	1000			**1200**
	2553.7	131.4	Enhanced rate of temperature change	450	43	1000			**1100**
	2571.6	132.4	Enhanced rate of temperature change	100	56	1000			**1100**
	2658.1	136.2	Beginning of temperature increase	440	101	1000			**1100**
North Atlantic									
ODP 980	1436.9	112.4	Temperature increase of D/O 25	130	50	1000[d]	1400[b]		**1800**
	1504.1	116.1	Temperature decrease during C26	220	80	1000[d]	1400[b]		**1800**
	1726.8	128.8	Final abrupt warming & CH_4 increase	350	170	400[e]		400	**700**
MD95-2042	2438.9	112.4	Temperature increase of D/O 25	450	50	500[d]	1400[b]		**1600**
	2486.0	116.1	Temperature decrease during C26	460	80	1000[d]	1400[b]		**1800**
	2570.0	128.8	Final abrupt warming & CH_4 increase	380	170	400[e]		400	**700**
	2650.5	131.8	Start of warming & CH_4 increase	360	280	1500[e]		400	**1700**
CH69-K09	1138.7	109.4	Temperature decrease following D/O 25	800	45	1000[d]	1400[b]		**1900**
	1181.1	116.2	Temperature decrease during C26	800	80	1000[d]	1400[b]		**1900**
	1268.8	128.8	Final abrupt warming & CH_4 increase	750	170	400[e]		400	**1000**
	1293.6	132.5	Benthic $\delta^{18}O$ decrease	750	340	1000	1700[f]		**2200**
Norwegian Sea									
MD95-2010	1246.1	116.1	Temperature decrease	520	80	1500	1400[b]		**2200**
	1260.4	128.8	Temperature increase	820	170	1500[e]		400	**1800**
Labrador Sea									
EW9302-JPC2	782.8	116.1	Temperature decrease	800	80	1500	1400[b]		**2300**
	839.3	128.8	Temperature increase & diatom mat	800	170	1500[e]		400	**1800**

See footnote on next page.

Footnote of Table 3:

[a] The total age uncertainty combines: (1) the resolution of correlated record (for example, the SST record from core MD02-2488, or the planktic $\delta^{18}O$ record from core MD95-2042); (2) the resolution of the reference record (e.g. δD or methane records from the EDC ice core, ice $\delta^{18}O$ record from NGRIP ice core); (3) the uncertainty derived from the matching procedure (graphically estimated when defining the tie-points with the Analyseries software, Paillard et al., 1996); and (4) for sediment cores from high northern latitudes only, the age uncertainty on the transfer of NGRIP record on EDC3 time scale (Capron et al., 2010) or the age uncertainty on the gas-ice age difference in EDC ice core (Loulergue et al., 2007).
[b] Capron et al. (2010)
[c] Loulergue et al. (2008)
[d] For these tie-points, the North Atlantic records have been correlated to the ice $\delta^{18}O$ record from the Greenland NGRIP ice core.
[e] For these tie-points, the North Atlantic records have been correlated to the methane record from the Antarctic EDC ice core.
[f] Because the tie-point has been defined by correlation to the benthic $\delta^{18}O$ record from core MD95-2042, the age uncertainty is that of core MD95-2042 on EDC3 time scale over the corresponding interval.

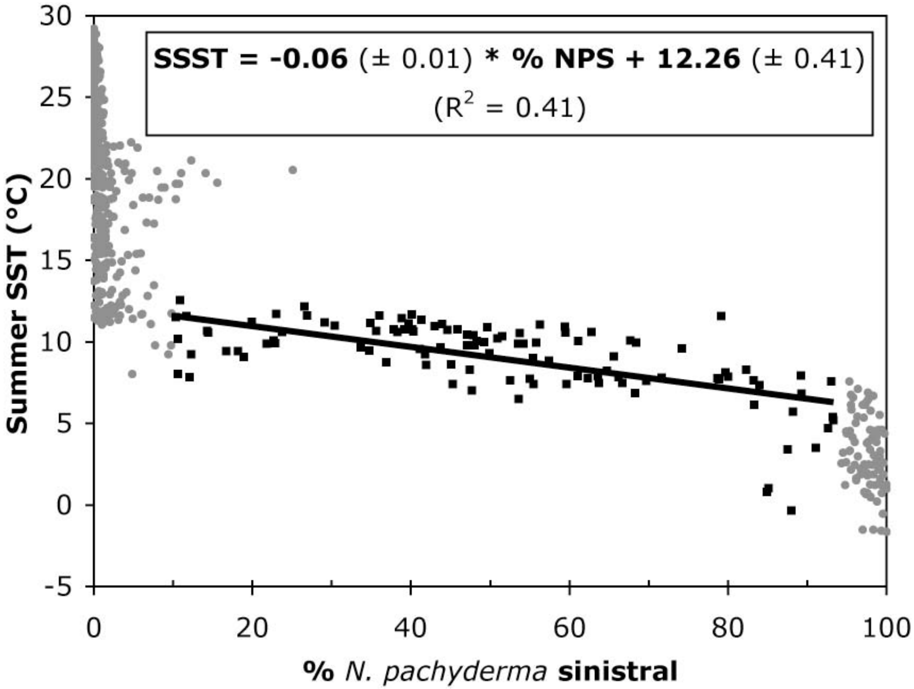

Fig. 1. Linear relationship defined between summer SST (SSST) and the percentage of the polar planktic species *Neogloboquadrina pachyderma* sinistral (NPS) in the North Atlantic (database from Kucera et al., 2005). The relationship (thick black line) is defined for % *N. pachyderma* sinistral between 10 % and 94 % and summer SST below 16 °C (black squares). Grey circles represent data characterized by % *N. pachyderma* sinistral above 94 % and below 10 %, or by SST values above 16 °C. The root mean square deviation of the relationship is ±1.8 °C (1 σ).

CPD
7, 3239–3286, 2011

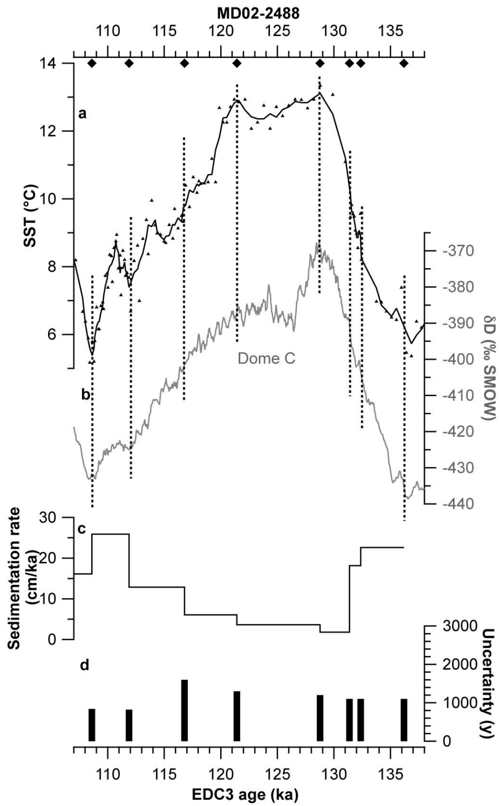

Fig. 2. Definition of the age model of core MD02-2488 from the Southern Ocean. **(a)** Sea Surface Temperature (3-point smoothing curve, black line) from core MD02-2488 (Govin et al., 2009). Diamonds and vertical dotted lines highlight the tie-points. **(b)** Antarctic EDC δD record (EPICA Community members, 2004; Jouzel et al., 2007) (5-point smoothing curve, grey line). **(c)** Sedimentation rate variations in core MD02-2488. **(d)** Age uncertainty of the tie-points defined between core MD02-2488 and EDC ice core (see Table 3 for details).

CPD
7, 3239–3286, 2011

Last Interglacial climate and ice sheet melting

A. Govin et al.

CPD
7, 3239–3286, 2011

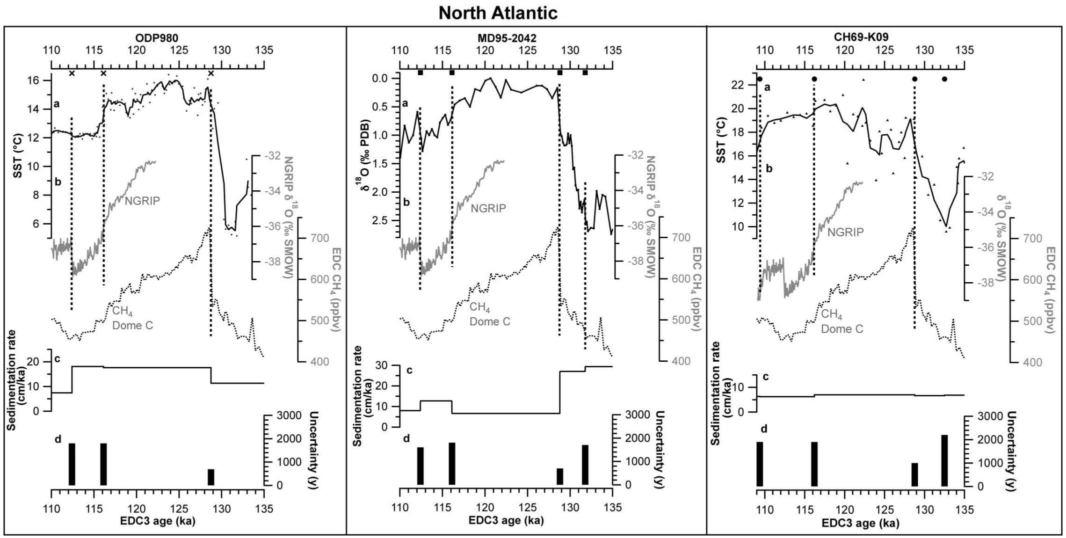

Fig. 3. Definition of the age model of the three sediment cores from the North Atlantic. **(a)** (left panel) Sea Surface Temperature (3-point smoothing curve, black line) from core ODP 980 (Oppo et al., 2006); (mid panel) planktic δ^{18}O record (black line) from core MD95-2042 (Shackleton et al., 2002); (right panel) Sea Surface Temperature (3-point smoothing curve, black line) from core CH69-K09 (Cortijo et al., 1999). **(b)** (all panels) Greenland NGRIP ice δ^{18}O record (North Greenland Ice Core Project members, 2004) (grey line) and Antarctic EDC methane record (Loulergue et al., 2008) (grey dotted line). **(c)** (all panels) Sedimentation rate variations. **(d)** (all panels) Age uncertainty of the defined tie-points (see Table 3 for details). Tie-points are indicated by symbols (crosses for core ODP 980, left panel; squares for core MD95-2042, mid panel; circles for core CH69-K09, right panel) and highlighted by the vertical dotted lines.

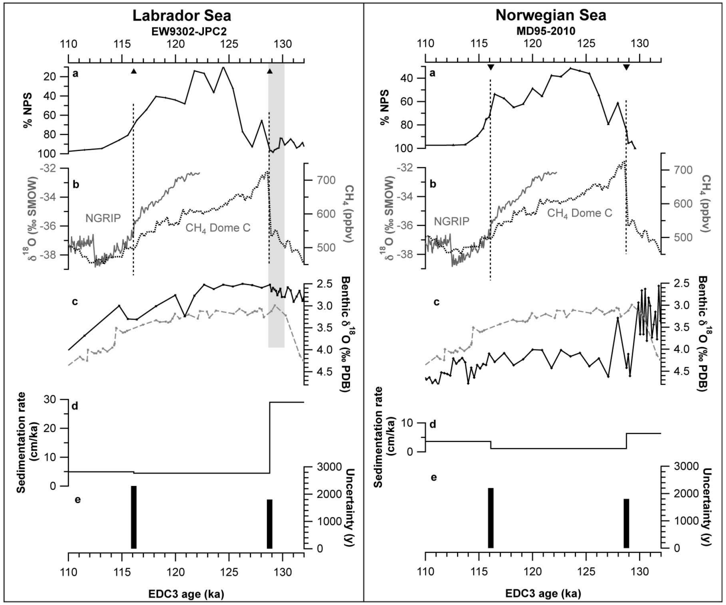

Fig. 4. Definition of the age model of the two cores from the Labrador Sea (left panel) and the Norwegian Sea (right panel). **(a)** Percentage of the polar species *N. pachyderma* sinistral (% NPS) (black line) from (left panel) core EW9302-JPC2 from the Labrador Sea (Rasmussen et al., 2003a), and (right panel) core MD95-2010 from the Norwegian Sea (Risebrobakken et al., 2005). **(b)** (all panels) Greenland NGRIP ice δ^{18}O record (North Greenland Ice Core Project members, 2004) (grey line) and Antarctic EDC methane record (Loulergue et al., 2008) (grey dotted line). **(c)** Benthic δ^{18}O record from (left panel) core EW9302-JPC2 (black line) (Rasmussen et al., 2003a) and from (right panel) core MD95-2010 (black line) (Risebrobakken et al., 2005), in comparison to the benthic δ^{18}O record of the North Atlantic core ODP 980 (grey dashed line) (Oppo et al., 2006). **(d)** (all panels) Sedimentation rate variations. **(e)** (all panels) Age uncertainty of the defined tie-points (see Table 3 for details). Tie-points are indicated by triangles in **(a)**, and highlighted by the vertical dotted lines. The grey shaded area in the left panel highlights the diatom mat at the onset of the LIG (Rasmussen et al., 2003a).

CPD
7, 3239–3286, 2011

Last Interglacial climate and ice sheet melting

A. Govin et al.

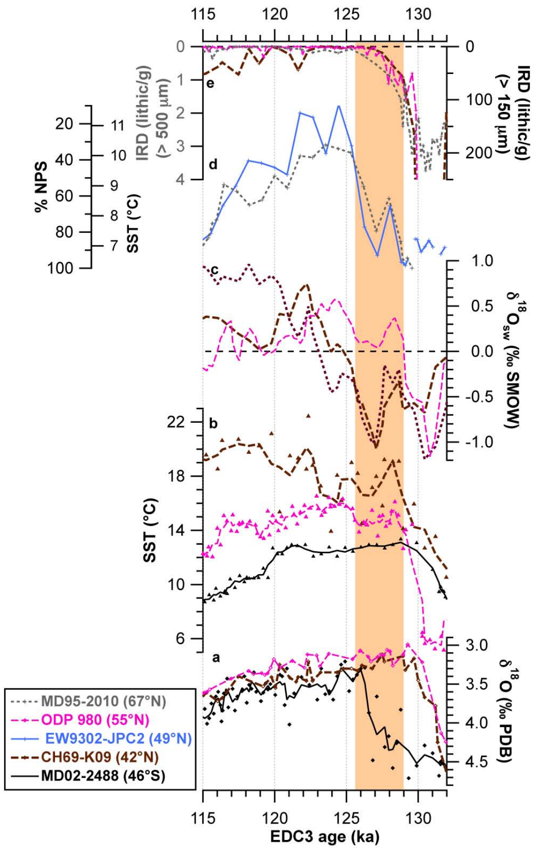

Fig. 5. Foraminiferal surface-water data over the period 131–115 ka. **(a)** Benthic $\delta^{18}O$, **(b)** summer SST, **(c)** seawater $\delta^{18}O$ ($\delta^{18}O_{sw}$), **(d)** percentage of the polar species *N. pachyderma* sinistral and **(e)** IRD records from the North Atlantic cores ODP 980 (dashed pink line) (Oppo et al., 2006) and CH69-K09 (dashed brown line) (Cortijo et al., 1999), the Norwegian Sea core MD95-2010 (dotted grey line) (Risebrobakken et al., 2006), the Labrador Sea core EW9302-JPC2 (Rasmussen et al., 2003a) (blue line), and the Southern Ocean core MD02-2488 (black line) (Govin et al., 2009). SST, seawater $\delta^{18}O$ records and Southern Ocean benthic records are 3-points smoothing curves. The red-shaded area highlights the period 129–125.5 ka of the early LIG (see text).

CPD
7, 3239–3286, 2011

Last Interglacial climate and ice sheet melting

A. Govin et al.

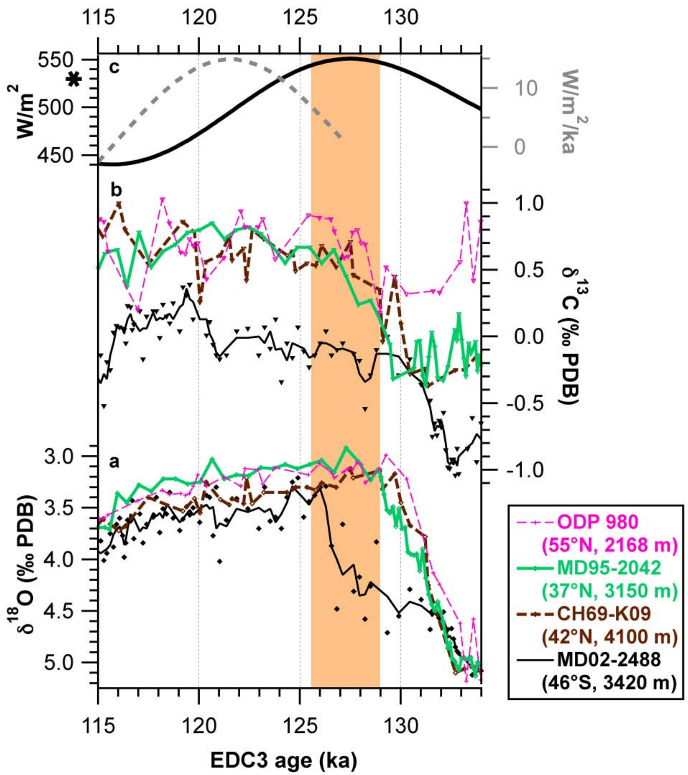

Fig. 6. Foraminiferal deep-water data over the period 134–115 ka. **(a)** Benthic δ^{18}O and **(b)** (*Cibicides*) δ^{13}C records from the North Atlantic cores ODP 980 (dashed pink line) (Oppo et al., 2006), MD95-2042 (green line) (Shackleton et al., 2002), CH69-K09 (dashed brown line) (Cortijo et al., 1999), and from the Southern Ocean core MD02-2488 (black line, 3-point smoothing curves) (Govin et al., 2009). **(c)** 21 June insolation at 65° N (black line, Berger, 1978). Corresponding rate of insolation change (dashed grey line, right y-axis) plotted for the period 127–115 ka only. The star along the left y-axis indicates the insolation maximum at 11 ka. The red-shaded area highlights the period 129–125.5 ka of the early LIG (see text).

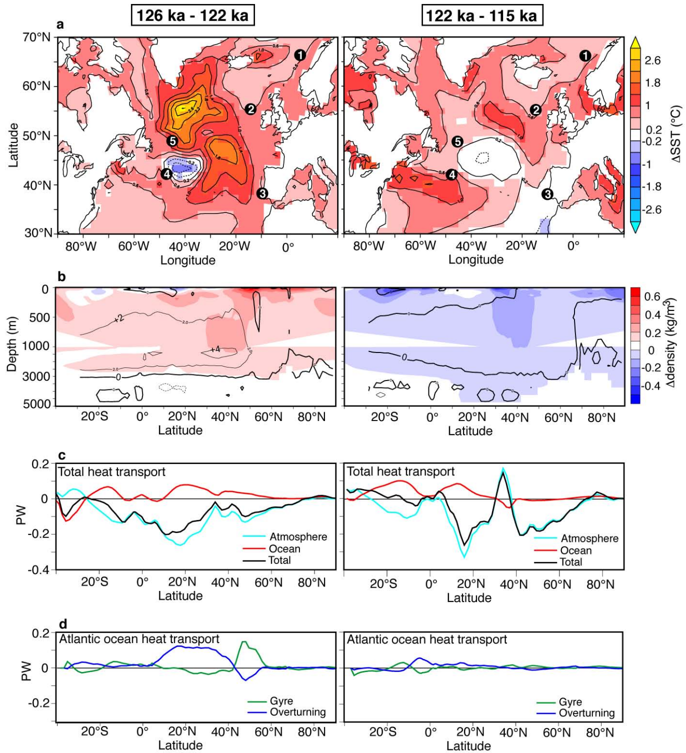

Fig. 7. Modeled climate response to insolation variations between (left panel) 126 and 122 ka, and (right panel) 122 and 115 ka. Averaged outputs over the last 100 years of the simulations are presented. We only show the statistically significant differences at the 95 % level using a student t-test on the interannual variability of the last 100 years of each simulation. **(a)** North Atlantic map of the mean annual SST anomalies. Black circles indicate the location of the northern sediment cores considered here: (1) MD95-2010 (Risebrobakken et al., 2006), (2) ODP 980 (Oppo et al., 2006), (3) MD95-2042 (Shackleton et al., 2002), (4) CH69-K09 (Cortijo et al., 1999), and (5) EW9302-JPC2 (Rasmussen et al., 2003a). **(b)** Atlantic annual mean zonal density (color scale) and overturning (2 Sv contour lines, flow is clockwise around positive contour lines) anomalies. **(c)** Total heat transport (black line, 1 PW = 10^{15} W), decomposed between the atmosphere (turquoise line) and the ocean (red line). **(d)** Atlantic Ocean heat transport decomposed into gyre (green line) and overturning (blue line) components.

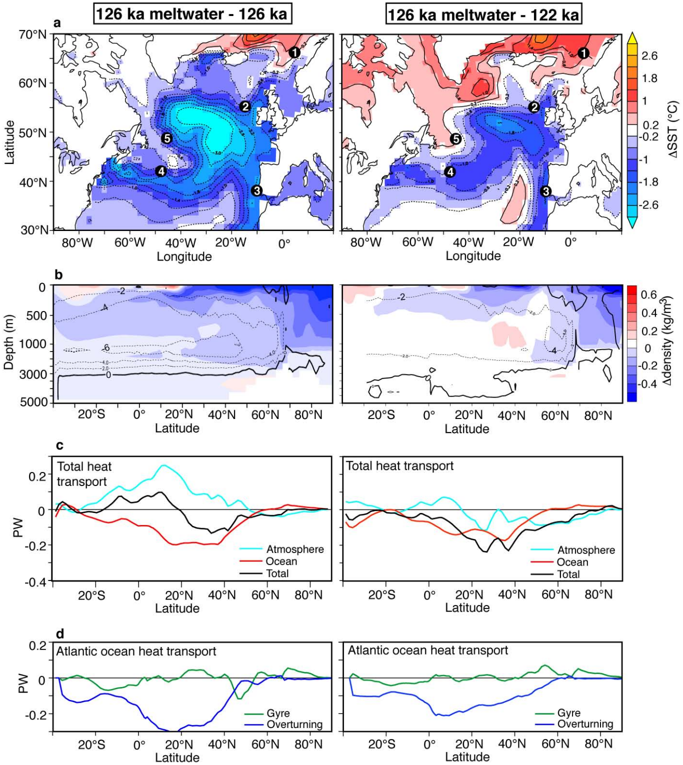

Fig. 8. Modeled climate response to the northern input of meltwater (left panel) at 126 ka with and without meltwater, and (right panel) between 126 ka with meltwater input and 122 ka. Averaged outputs over the last 100 years of the simulations are presented. We only show the statistically significant differences at the 95 % level using a student t-test on the interannual variability of the last 100 years of each simulation. **(a)** North Atlantic map of the mean annual SST anomalies. Black circles indicate the location of the northern sediment cores considered here: (1) MD95-2010 (Risebrobakken et al., 2006), (2) ODP 980 (Oppo et al., 2006), (3) MD95-2042 (Shackleton et al., 2002), (4) CH69-K09 (Cortijo et al., 1999), and (5) EW9302-JPC2 (Rasmussen et al., 2003a). **(b)** Atlantic annual mean zonal density (color scale) and overturning (2 Sv contour lines, flow is clockwise around positive contour lines) anomalies. **(c)** Total heat transport (black line, 1 PW = 10^{15} W), decomposed between the atmosphere (turquoise line) and the ocean (red line). **(d)** Atlantic Ocean heat transport decomposed into gyre (green line) and overturning (blue line) components.

CPD
7, 3239–3286, 2011